# SPECTRAL DECOMPOSITION USING S-TRANSFORM FOR HYDROCARBON DETECTION AND FILTERING

A Thesis

by

ZHAO ZHANG

Submitted to the Office of Graduate Studies of
Texas A&M University
in partial fulfillment of the requirements for the degree of

MASTER OF SCIENCE

August 2011

Major Subject: Geophysics

Spectral Decomposition Using S-transform for Hydrocarbon Detection and Filtering

# SPECTRAL DECOMPOSITION USING S-TRANSFORM FOR HYDROCARBON DETECTION AND FILTERING

A Thesis

by

ZHAO ZHANG

Submitted to the Office of Graduate Studies of
Texas A&M University
in partial fulfillment of the requirements for the degree of

MASTER OF SCIENCE

Approved by:

| | |
|---|---|
| Chair of Committee, | Yuefeng Sun |
| Committee Members, | Luc T. Ikelle |
| | Deepa Kundur |
| Head of Department, | Andreas Kronenberg |

August 2011

Major Subject: Geophysics

# ABSTRACT

Spectral Decomposition Using S-transform for

Hydrocarbon Detection and Filtering.

(August 2011)

Zhao Zhang, B.S., Tianjin University

Chair of Advisory Committee: Dr. Yuefeng Sun

Spectral decomposition is a modern tool that utilizes seismic data to generate additional useful information in seismic exploration for hydrocarbon detection, lithology identification, stratigraphic interpretation, filtering and others. Different spectral decomposition methods with applications to seismic data were reported and investigated in past years. Many methods usually do not consider the non-stationary features of seismic data and, therefore, are not likely to give satisfactory results. S-transform developed in recent years is able to provide time-dependent frequency analysis while maintaining a direct relationship with the Fourier spectrum, a unique property that other methods of spectral decomposition may not have. In this thesis, I investigated the feasibility and efficiency of using S-transform for hydrocarbon detection and time-varying surface wave filtering.

S-transform was first applied to two seismic data sets from a clastic reservoir in the North Sea and a deep carbonate reservoir in the Sichuan Basin, China. Results from

both cases demonstrated that S-transform decomposition technique can detect hydrocarbon zones effectively and helps to build the relationships between lithology changes and high frequency variation and between hydrocarbon occurrence and low-frequency anomaly. However, its time resolution needs to be improved.

In the second part of my thesis, I used S-transform to develop a novel Time-frequency-wave-number-domain (T-F-K) filtering method to separate surface wave from reflected waves in seismic records. The S-T-F-K filtering proposed here can be used to analyze surface waves on separate f-k panels at different times. The method was tested using hydrophone records of four-component seismic data acquired in the shallow-water Persian Gulf where the average water depth is about 10m and Scholte waves and other surfaces wave persistently strong. Results showed that this new S-T-F-K method is able to separate and attenuate surface waves and to improve greatly the quality of seismic reflection signals that are otherwise completely concealed by the aliased surface waves.

# DEDICATION

To my parents, who were not lucky enough to have much education when they were growing up, but value education most highly

# ACKNOWLEDGMENTS

The completion of a master's degree is an endeavor that requires much outside help, especially for a person like me who transferred from computer science to geophysics. Consequently, I owe many debts of gratitude. First and foremost, I would like to thank my father, Qingtong Zhang, and my mother, Caifeng Wang. They have always been my comforters, although we have not always been able to be together on a daily basis in recent years.

Secondly, I thank Dr. Sun, the chairman of my advisory committee, for his helpful advice and comments throughout my master's program at Texas A&M University and for the review of this thesis. His expertise on geophysics and computer skills have greatly enhanced my research. His quick thinking always amazes me. His sincerity toward science and teaching will always set an example for many to follow. As an advisor, Dr. Sun has been very open to what I'd like to do. He introduced me to the seismic data processing and provided me financial support.

I am very grateful to my other committee members: Dr. Ikelle and Dr. Kundur. Dr. Ikelle is always there to encourage me, even when I doubted of myself on the sharp learning curve in geophysics. He has given me valuable advice that will be of great value throughout my entire life. I learned a lot from Dr. Kundur's classes. She introduced me to the field of digital signal processing and gave me important guidance during my first steps into data processing studies. Her clear explanations made the course easy to follow and helped me build my academic confidence. More importantly, she sets an example for

me on how women can success in science and engineering.

I wish to express my warm and sincere thanks to Dr. Bruce Herbert, assistant department head, for his instruction on how to communicate with different people, and for his help on recommendations. My sincere thanks are due to the department staffs: Debbie Schorm, Sandra Dunham and Shelly Peacock. They all gave me a lot of help on the steps to graduation.

I am grateful to China Petroleum & Chemical Corporation for providing the data and financial support.

During my two years at Texas A&M University, I have been lucky to work with several talented and kind graduate student fellows such as (in alphabetic order): Hamid Adesokan, Jingyi Li, Qifeng Dou, Tom Hull, Meng Xue, Tingting Zhang, Yong Zhang and Lijing Zou. They (and often their families) have all provided assistance to me in many aspects of my studies and in my life, even though they are all extremely busy. I also thank my friends in China, such as Bowen Ding, Dahe Zhang, Jingwei Liu, Feng Xiao, Mingxi Hu, Qi Zhang, Shanchan Zhao, Wei Zhou, Wei Wei and Yin Sun. They always bring me happiness and comfort through the Internet and share some of the happiest memories. There is a lightness of heart that comes from just telling them about my day and listening to theirs. They've stood by me through life's ups and downs.

# TABLE OF CONTENTS

Page

Page

# LIST OF FIGURES

Page

Page

# 1. INTRODUCTION

Seismic data is difficult to interpret for reservoir properties and fluid detection. However, in some cases, the spectral analysis can open the door for a better seismic interpretation. The frequency-domain representation of a time series often illustrates stratigraphic and structural details that are difficult to visualize in the time domain. Lithology and pore fluid shows a significant difference in the frequency domain. Thus, spectral analysis research has gained considerable momentum in recent years.

In addition, spectral analysis offers new opportunities for improved processing algorithms and spectral interpretation methods. Strong surface-wave occurrence and its dispersion create severe problems for seismic data analysis in the shallow water environment of the Persian Gulf where the average water depth is about 10 to 15m. Common technique for surface-wave analysis is f-k filtering based on exploiting low frequency and high-amplitude characteristics. However, spatial aliasing of surface waves due to under-sampling presents unique challenges to these methods. With the help of wave-number spectral analysis, different seismic events could be separated and extracted.

In this study, I first propose a conceptual description of S-transform based on the spectral analysis method. I then illustrate the improvement in spectral resolution through synthetic signals and real data sets. Further, an S-transform based t-f-k transform is

---

This thesis follows the style of Geophysics.

established. It allows the dynamic analysis of the surface-wave spectrum over time. Results of my studies are expected to be useful for reservoir quality prediction and for optimization of reservoir development strategies.

### 1.1 Objectives

The first objective of this research is to investigate a new method to implement time-frequency decomposition that would help establish possible relationship between different seismic events and frequency distribution related to hydrocarbon occurrence and lithology changes. The second objective is to demonstrate the application of the S-transform and T-F-K transform for surface waves analysis.

### 1.2 Literature Review

Dilay and Eastwood (1995) firstly applied spectral analysis to seismic monitoring of thermal recovery. Peyton et al. (1998) then implemented spectral decomposition and coherency on 3D data to interpret complex incised valleys system. Partyka et al. (1999) further used windowed spectral analysis to produce discrete-frequency energy cubes for reservoir characterization. He illustrated that spectral decomposition can be a powerful aid to the imaging and mapping of bed thickness and geologic discontinuities. Castagna et al. (2003) and Castagna and Sun (2006) showed that spectral decomposition could help in detection of hydrocarbons under certain circumstances. He used Instantaneous spectral analysis (ISA) method which had a much better combination of temporal and frequency resolution than conventional spectral decomposition methods. He also

indicated that low-frequency shadows were much more apparent on spectrally decomposed data than on seismic sections.

For the methods of spectral decomposition, the widely used short-time Fourier transform (STFT) method was introduced by Cohen (1995). In STFT, time-frequency resolution is fixed over the entire time-frequency space by preselecting a window length. Instead of producing a time-frequency spectrum, the continuous-wavelet transform (CWT) produces a time-scale map called a scalogram (Daubechies, 1992). Hlawatsch and Boudreaux-Bartels (1992) took scale to be inversely proportional to the center frequency of the wavelet and represented the scalogram as a time-frequency map.

Recently, Stockwell et al. (1996) introduced the S-transform as a tool for optimal time-frequency analysis of geophysical signals. It is an invertible time-frequency spectral localization technique that combines elements of wavelet transforms and short-time Fourier transforms.

Several authors implemented S-transform in spectral analysis. Deng et al. (2007) implemented spectral decomposition techniques to stack seismic section from deepwater reservoir. His results showed that gas associated spectral anomalies occurs at both low-frequency or high-frequency iso-frequency sections. Zhu et al. (2003) and Goodyear et al. (2004) provided the method for processing magnetic resonance signal data.

Embree et al. (1963) firstly used the term velocity filter in data processing. Wiggins (1976) called these two-dimensional operators w-k filters. When applied to two-dimensional arrays of seismometers such operators are usually called beam forming filters. Foster et al. (1964) and Schneider et al. (1965) continued filter design using the

Wiener-Hopf optimum filter theory. These methods are generally more elaborated and are used to de-ghost seismic records and to reduce multiple reflections. Velocity filters may operate in the digital domain as above, or, equally effectively, in the analog domain with the use of laser sources and optical processing.

Studies on surface waves attenuation have been taken for many years. Nawab and Quatieri (1988) firstly used time windowing and short-time Fourier transform. There exists a compromise between window sizes and frequency precision, thus the performance of the filter is frequency dependent. Beresford-Smith and Rango (1989) proposed a method that combined windowing in the time-offset domain and f-k filtering together. However, it was computationally expensive. S-transform is also implemented in filtering design. Recently, Pinnegar and Eaton (2003) designed pre-stack noise attenuation filtering system based on S-transform. Askari and Siahkoohi (2007) discussed S-transform to attenuate the influence of ground roll waves.

### 1.3 Thesis Structure

This study presents a new methodology for computing a time-frequency map of non-stationary signals using the S-transform with application to hydrocarbon detections and surface wave analysis.

In the first section, I introduced some geological and geophysical fundamentals about the research and the challenges that we have encountered.

In Section II, I will discuss the spectral decomposition methods in this study. S-transform is compared with other two traditional methods. Then two field data sets are

used to test the method. For the first data set from North Sea, I will focus on detecting the bright spot in the time-frequency domain. For the second data set from Sichuan Basin, I will use the spectral decomposition to predict the lithology changing.

In Section III, a new surface-wave filtering method based on S-transform is investigated and testified. I will first discuss the challenges in the shallow water environment. Comparing with traditional methods, I decompose the signal into the time-frequency-wavenumber domain which is easier for us to define the reject zones.

In Section IV, the summarization of my study and my further research plan will be given.

# 2. SPECTRAL DECOMPOSITION USING S-TRANSFORM

Over the past two decades, continuous wavelet-transform (CWT) and short-time Fourier transform (STFT) have been applied to spectral decomposition. Due to the fixed width of the STFT window, low frequencies are hard to detect and high frequencies bring poor time resolution. Improved performance is observed when applying the CWT, but it also produces time-scale plots that are unsuitable for intuitive visual analysis.

In this section, S-transform is compared with STFT and CWT. Then the spectral analysis method based on S-transform is tested on two real datasets.

## 2.1 Decomposition Methods

Seismic data which has spectral content varying significantly with time is considered non-stationary and requires nonstandard methods of decomposition. Various techniques have been utilized in time-frequency analysis. Traditionally, the short-time Fourier transform (STFT) and continuous-wavelet transform (CWT) have been applied. This section will review these two methods and introduce another novel approach for time-frequency analysis.

### 2.1.1 Basic Concepts

Since the beginning of the history of digital recording, geophysical data processors have decomposed the measured seismic signal into Fourier components. Any time series can be represented uniquely as a linear combination of other harmonic time

series in Fourier analysis.

Fourier analysis simply decomposes the seismic data into a term of sines and cosines at predetermined frequencies. Amplitude and phase can be expressed in terms of sines and cosines. We also could express the cross-correlation coefficients of amplitude and phase of these harmonics with the data used as a complex number,

$$A(\omega) = a(\omega)e^{i\Phi(\omega)}.$$

The Fourier transform F( $\omega$ ) of a signal f(t) is the inner product of the signal with the basis function $e^{i\omega t}$,

$$f\ \omega\ =\ \int_{-\infty}^{\infty} f\ t\ e^{-i\omega t} dt\ .$$

Research focuses more on the amplitude component of the spectrum. Different amplitudes on specific frequency can show the stratigraphic configuration, although phase is equally or more important.

Both the STFT and CWT is base on Fourier analysis. They differ from each other in the applications of their respective tapers. For the STFT, the tapers are independent of frequencies and are the same for all sines and cosines. For CWT, the tapering windows are proportional to the frequencies of the sines and cosines and are shorter for higher frequencies.

### 2.1.2 Short-time Fourier Transform

The Fourier transform gives the overall frequency behaviors for the entire signal. It is inadequate for analyzing non-stationary signals, such as seismic signals. We can include the time dependence by windowing the signal (i.e. taking short segments of the

signal) and then performing the Fourier transform on the windowed data to obtain local frequency information. Such approach of time frequency analysis is called short-time Fourier transform (STFT) and the time frequency map is called a spectrogram (Cohen, 1995). The STFT is given by the inner production of the signal f (t) with a time shifted window function$\emptyset\ t$ . Mathematically, it can be expressed as:

$$\text{STFT}\ \omega,\tau\ =\ \ \ f\ t\ \emptyset(t-\tau)e^{-i\omega t}dt\ ,$$

where the window function $\emptyset$ is centered at time t = $\tau$ and $\emptyset$ can be complex (Cohen, 1995).

### 2.1.3 Continuous-wavelet Transform

The continuous wavelet transform (CWT) is an alternative method to analyze a signal. It is defined as the sum over all time of the signal f (t) multiplied by a scaled and shifted version of the analyzing wavelet function. Mathematically, it is defined as the inner product of a family of wavelets $\varphi_{\sigma,\tau}\ \tau$ with signal f (t):

$$F_w\ \sigma,\tau\ =\ \ \int_{-\infty}^{\infty} f(t)\frac{1}{\sqrt{\sigma}}\varphi\ \ \frac{t-\tau}{\sigma}\ \ dt,$$

$F_w\ \sigma,\tau$ is the time-scale map (i.e. the scalogram).

The wavelet $\varphi\ \ t$ is localized in both time and frequency:

$$\varphi_{\sigma,\tau}\ \tau\ =\ \frac{1}{\sqrt{\sigma}}\varphi\ \ \frac{t-\tau}{\sigma}$$

where $\sigma,\tau \in R$ (real number) and $\sigma \neq 0$. $\sigma$ is called the dilation parameter or scale and $\tau$ is called the translation parameter. The main purpose of using the mother wavelet is to provide a source function to generate the daughter wavelets (Miao and Cheadle, 1998) which are simply the translated and scaled versions of the mother wavelet (Miao

and Moon, 1994).

Unlike Fourier transform, the continuous wavelet transform possesses the ability to construct a time-frequency representation of a signal that offers time and frequency localization.

### 2.1.4 S-Transform

The S-transform can conceptually be viewed as a hybrid of short-time Fourier analysis and wavelet analysis. It is defined as:

$$S_x(t, f) = \int_{-\infty}^{+\infty} u(\tau) w(t-\tau, \sigma(f)) \exp(-j2\pi f\tau) d\tau$$

with a constraint (Stockwell et al., 1996):

$$\int_{-\infty}^{+\infty} w(t-\tau, \sigma(f)) d\tau = 1 .$$

The $w(\tau, f)$ is the Gaussian window:

$$w(t, \sigma(f)) = \frac{1}{\sigma(f)\sqrt{2\pi}} \exp(-\frac{t^2}{2\sigma^2(f)})$$

where t is the time, $f$ is the frequency variables, and $\tau$ is a parameter that controls the position of the Gaussian window along the t axis. $\sigma(f)$ is defined as

$$\sigma(f) = \frac{1}{f} .$$

The S spectrum is invertible and the inverse transform algorithm is defined (Stockwell, 1996) as:

$$u(t) = \int_{-\infty}^{+\infty} \left[ \int_{-\infty}^{+\infty} S(\tau, f) d\tau \right] \exp(j2\pi f t) df .$$

The similarity between S-transform and STFT is that they are both derived from

the Fourier transform of the time series multiplied by a time-shift window (Stockwell, 1996). However, unlike STFT, the standard deviation $\sigma(f)$ in S-transform is actually a function of frequency. Consequently, the window function is also a function of time and frequency. As the width of the window is dictated by the frequency, it is apparent that the window is wider in the time domain at lower frequencies which means the window provides good localization in the frequency domain for low frequencies (Stockwell, 2006). Due to the low frequency spectrum of surface wave, this aspect makes S-transform more appropriate for further analysis.

In both S-transform and CWT, the window size changes with both time and frequency. However, the wavelet used in S-transform does not satisfy the condition of zero mean for an admissible wavelet. The oscillatory parts of the S-transform wavelet are provided by the complex Fourier sinusoid, which does not translate with the Gaussian window when $\tau$is changed (Pinnegar and Mansinha, 2003). As a result, the shapes of the real and imaginary parts of the S-transform wavelet change when Gaussian window translates in time. Comparing to S-transform, the shape of wavelet of CWT is consistent.

S-transform combines progressive resolution with absolutely referenced phase information (Stockwell, 2006). Therefore it could estimate the local amplitude spectrum and the local phase spectrum. Also, it is sampled at the discrete Fourier transform frequencies (Stockwell, 2006). The test examples also show S-transform brings a better imagine than traditional transforms.

## 2.2 Spectral Decomposition

Spectral decomposition techniques typically generate a continuous volume of instantaneous spectral attributes from seismic data, to provide useful information for reservoir characterization and direct hydrocarbon detection.

The low frequency shadows are used as hydrocarbon indicators. The shadow is probably coming from high-frequency attenuation in the reservoir itself (Dilay and Eastwood 1995, Mitchell et al., 1997), so that the local domain frequency moves toward the low-frequency range. However, it is often difficult to explain observed shadows under thin reservoir where there are insufficient travel paths through absorbing gas reservoir to justify the observed shift of spectral energy from high to low frequencies (Castagna et al., 2002). One possible explanation is that these are locally converted shear waves that have traveled mostly as P-waves and thus arrive slightly after the true primary event (Castagna et al., 2002). Ebrom (2004) listed about ten possible mechanisms reasons explaining this problem. It is believed that these shadows are caused by at least one of these mechanisms.

The optimal time-frequency resolution property of the S-transform makes it useful in seismic data analysis. High-frequency resolution at low frequencies helps to detect these low frequency shadows.

For a 2-D seismic section, the spectral analysis based on S-transform involves the following steps:

1) Decompose each trace into frequency components using the S-transform method to produce the frequency variation basing on specific time.

2) Sort the frequency information of all traces in the time-frequency domain to produce frequency cubes.
3) Pick up the two-dimensional frequency data based on specific frequency. The horizontal axis represents location and the vertical represents time.

We can see, after the processing, the 2D seismic section becomes a time, frequency and distance (trace position) cube. To interpret this data, the interpreter should analyze the iso-frequency panels along the frequency axis to search for geological features that gives rises to anomalous spectral amplitudes. For 3D data, spectral decomposition is applied in a time window that bounds a zone of interest. Interpretation is then done in the generated frequency slice.

**2.3 Synthetic Test**

In order to evaluate the suitability of the proposed approach, we first carry out the test with a synthetic signal. The signal is the summation of three cosine functions of frequencies of 0.5, 1, and 3 Hz (Figure 1). The lowest frequency starts at 14 sec and lasts for 5 sec. The cosine functions of 1 and 3 Hz start at 13 sec and last to 18 and 16 sec, respectively. The equation of the testing single is shown as following:

$$F(t) = \begin{cases} \cos(1*2\pi t) + \cos(3*2\pi t) & 13 \le t < 14 \\ \cos(0.5*2\pi t) + \cos(1*2\pi t) + \cos(3*2\pi t) & 14 \le t < 16 \\ \cos(0.5*2\pi t) + \cos(1*2\pi t) & 16 \le t < 18 \\ \cos(0.5*2\pi t) & 18 \le t < 19 \\ 0 & otherwise \end{cases}$$

The S-transform of the synthetic signal is shown in Figure 2 and highlighted area

shows the multi-frequency content of the signal and the occurrence in time of the different cosine functions. The expected better frequency resolution of the low-frequency component and the better time resolution of the high-frequency signals are also shown.

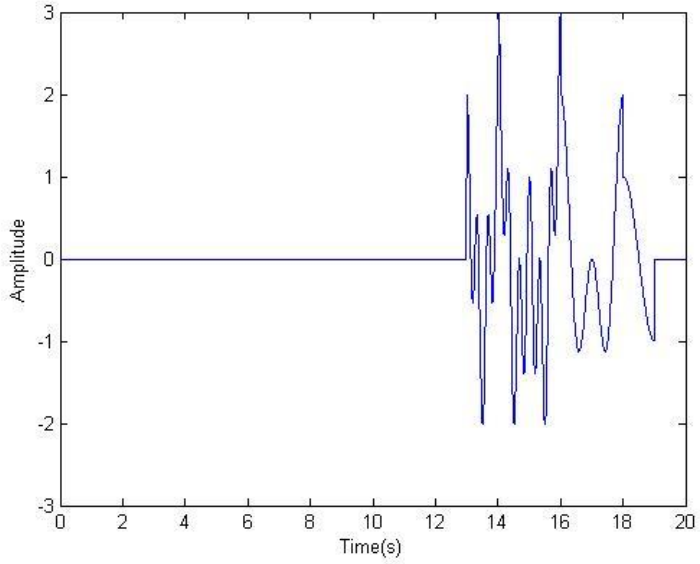


Figure 1 Synthetic trace composed of three wavelets with different frequencies and temporal locations

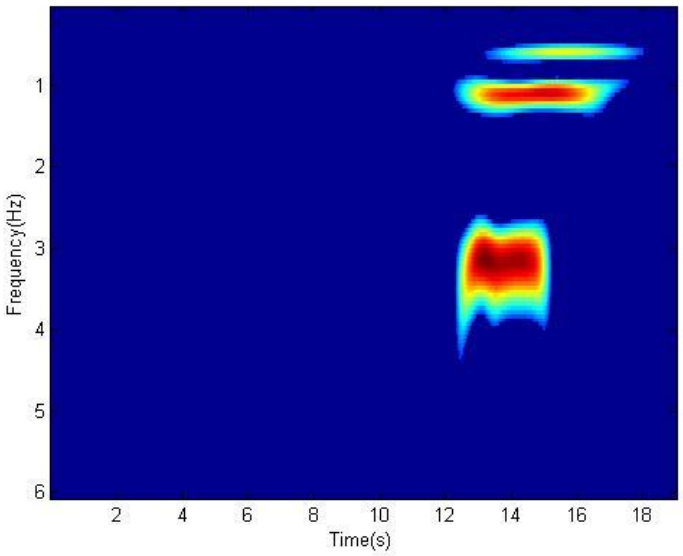


Figure 2 Time-frequency distribution of the synthetic trace

## 2.4 Application to Seismic Data

We apply the S-transform to real data to demonstrate how to detect hydrocarbon in time-frequency domain. My test data is from two different locations.

### 2.4.1 Example 1: North Viking Graben

The first reservoir studied is from the North Viking Graben area in the northern North Sea Basin (Figure 3, Figure 4). It was formed as a result of late Permian to Triassic rifting and trends north-northeast.

It has been demonstrated that the major oil and gas accumulations in the northern North Sea have been trapped in the Tertiary sandstones, which were formed within certain fine-grained, organic-carbon-rich marine strata of late Jurassic and earliest Cretaceous age. And the depositional environment types include fluvial, deltaic and shallow marine. The reservoir intervals are formed by coarse clastic sedimentary rock

and separated by deep water shale. (USGS, 2010)

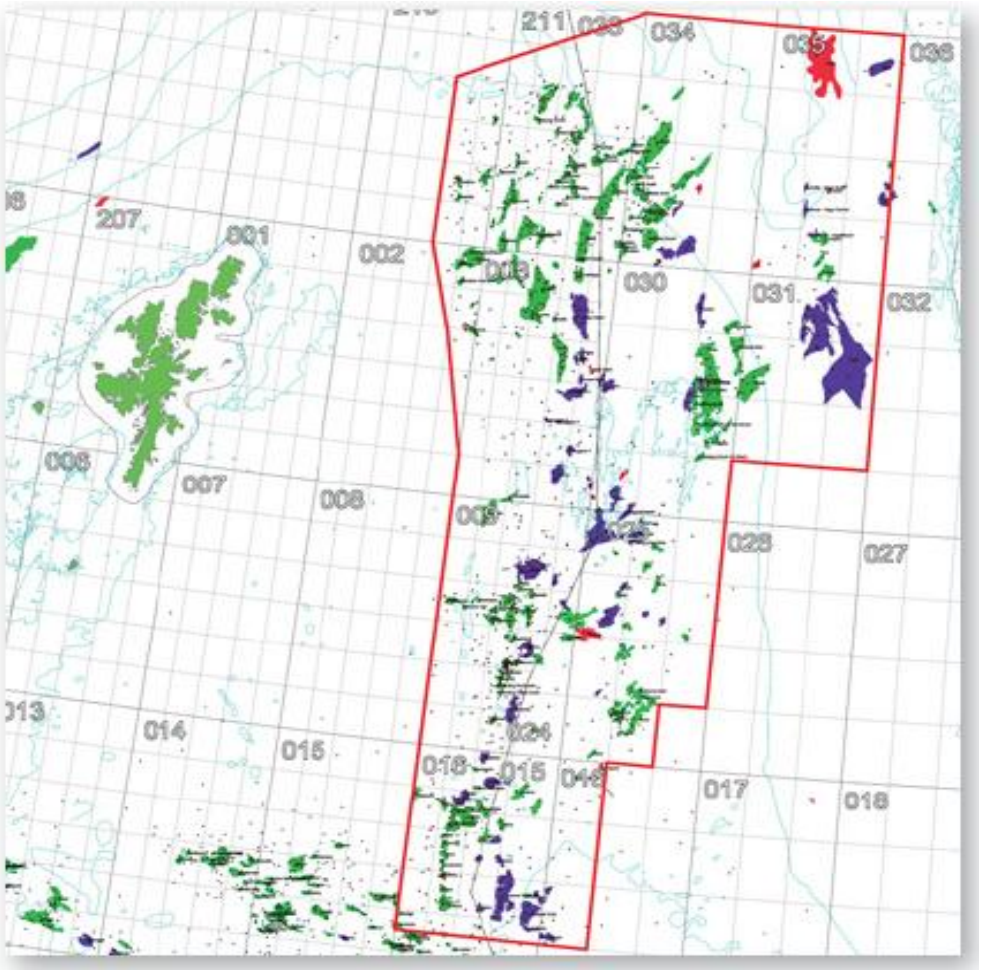


Figure 3 Location of studied area in the North Sea (USGS, 2010)

In this section, two wells will be used to verify this method. Well A is Jurassic age clastic sediments which range in depositional environments from fluvial to deltaic and shallow marine. Well B is the Paleocene deep water clastics. The Paleocene interval is undisturbed by the rift tectonism and dips gently into the basin.

Figure 5 shows the seismic line which consists of 1001 shot records and orients in a structural dip direction. Each shot record consists of 120 channels for six seconds. The seismic data are sampled every four milliseconds. Well A intersects the seismic line at shot-point 440 (CDP NO.808) and Well B is located at shot-point 822 (CDP NO. 1572).

Based on the references published by Exxon Mobile (Keys and Foster, 1998), a significant unconformity occurs at the base of the Cretaceous, which is located at the approximately 1.97 second two-way travel-time in Well A and 2.46 second two-way travel-time in Well B (Figure 5). Jurassic syn-rift sediments are overlain by Cretaceous and Tertiary basin fills.

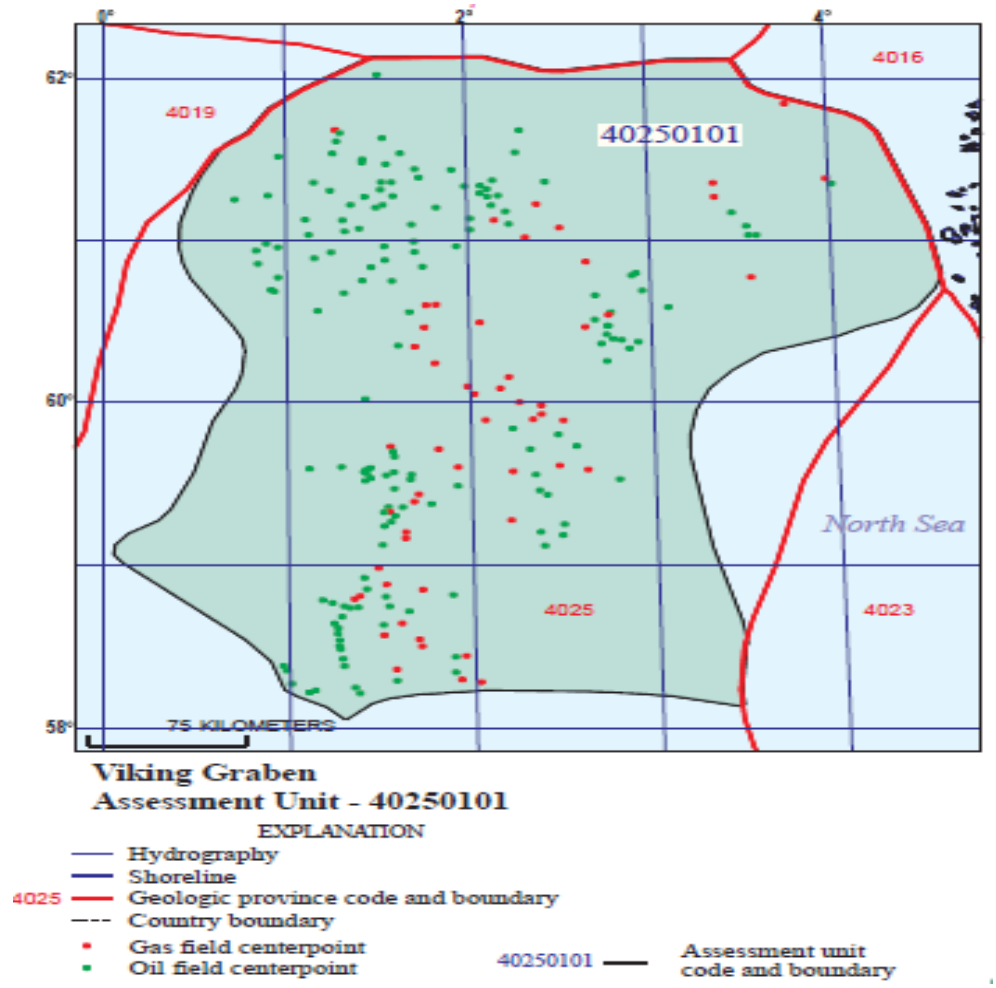


Figure 4 Overview of hydrograph of studied area in the North Sea (USGS, 2010)

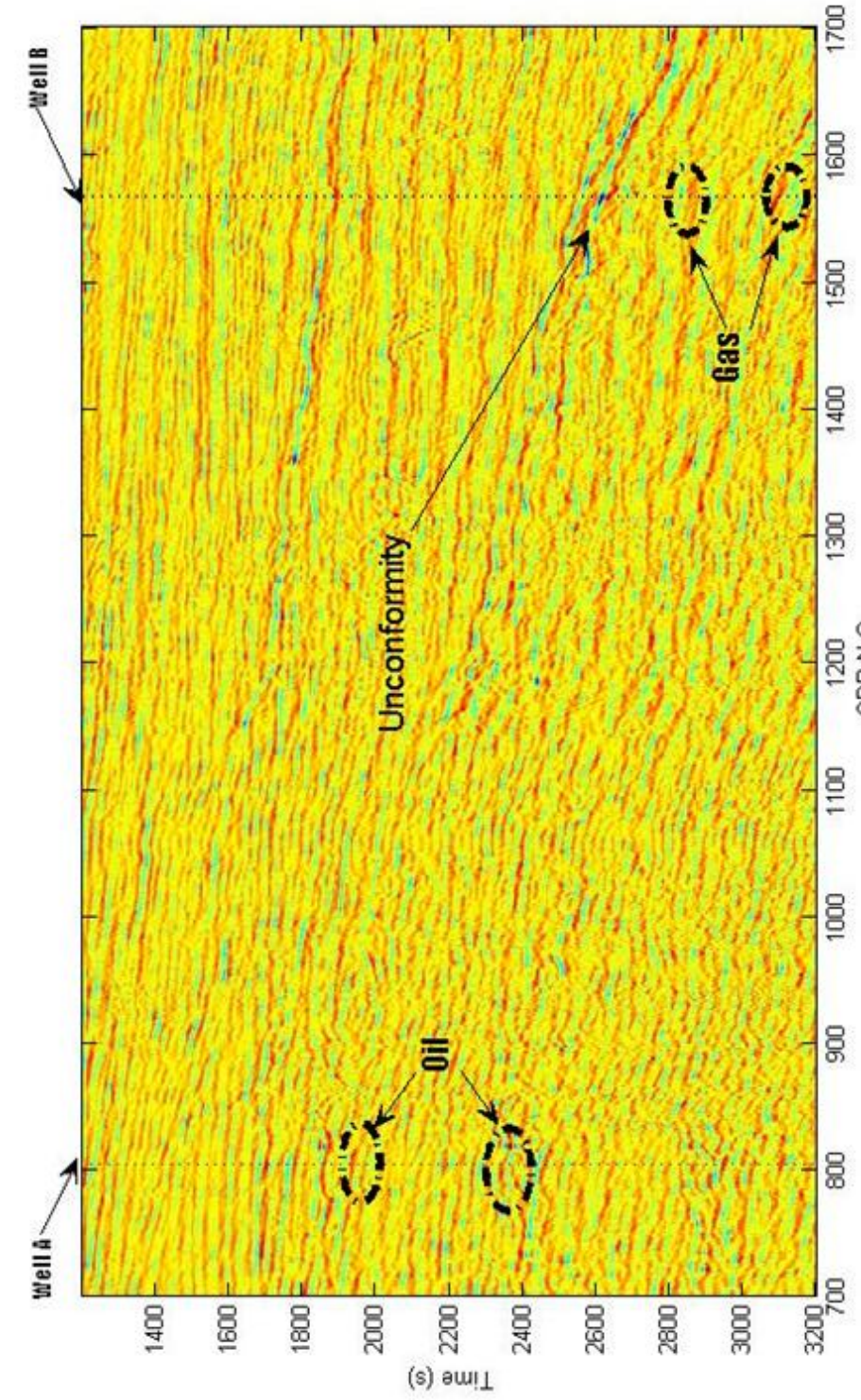


Figure 5 2-D seismic section of studied area in the North Sea

#### 2.4.1.1 Synthetic Data

In this section, the synthetic example will be presented to tie time with depth. In this study, only primary seismic waves are generated in synthetic seismic trace without multiples. Moreover, the log data provides data with a sampling interval that is smaller than the vertical resolution of the seismic data. So the S-transform decomposition will be first applied to the synthetic trace to verify its validity. The relationship between well log data and the true seismic data will be clearly revealed by the seismic trace at the well location.

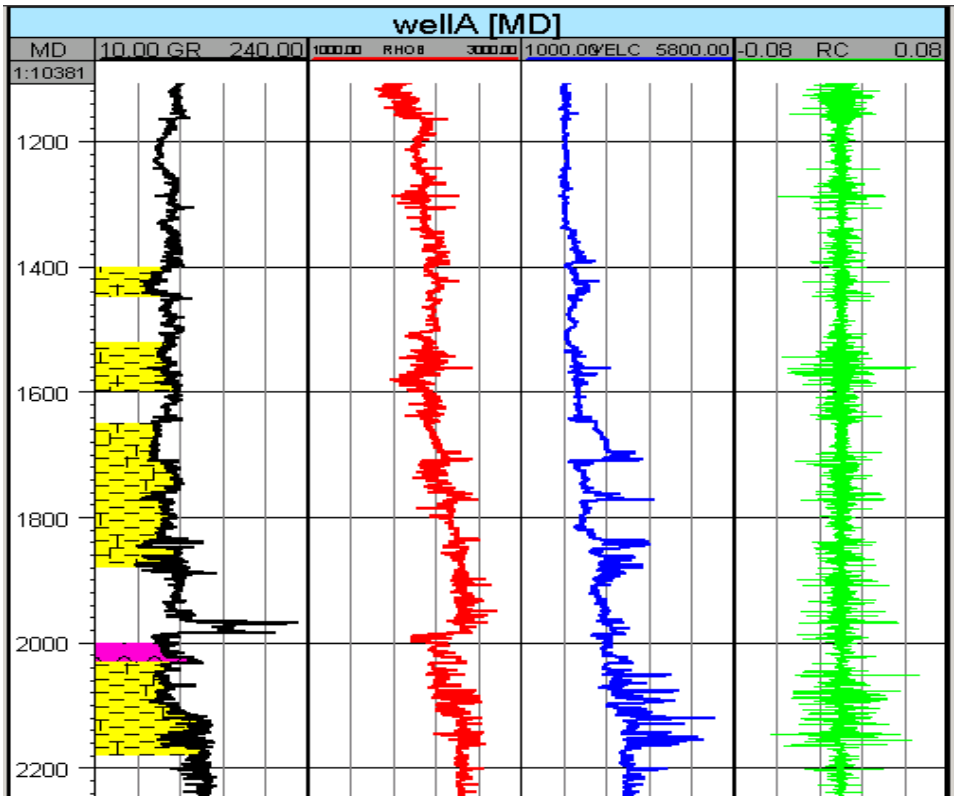


Figure 6 Synthetic data trace construction based on depth, from left to right: (a) Gamma Ray (yellow- oil zone, pink – gas zone) (b) Density (c) Velocity (d) Reflection coefficient

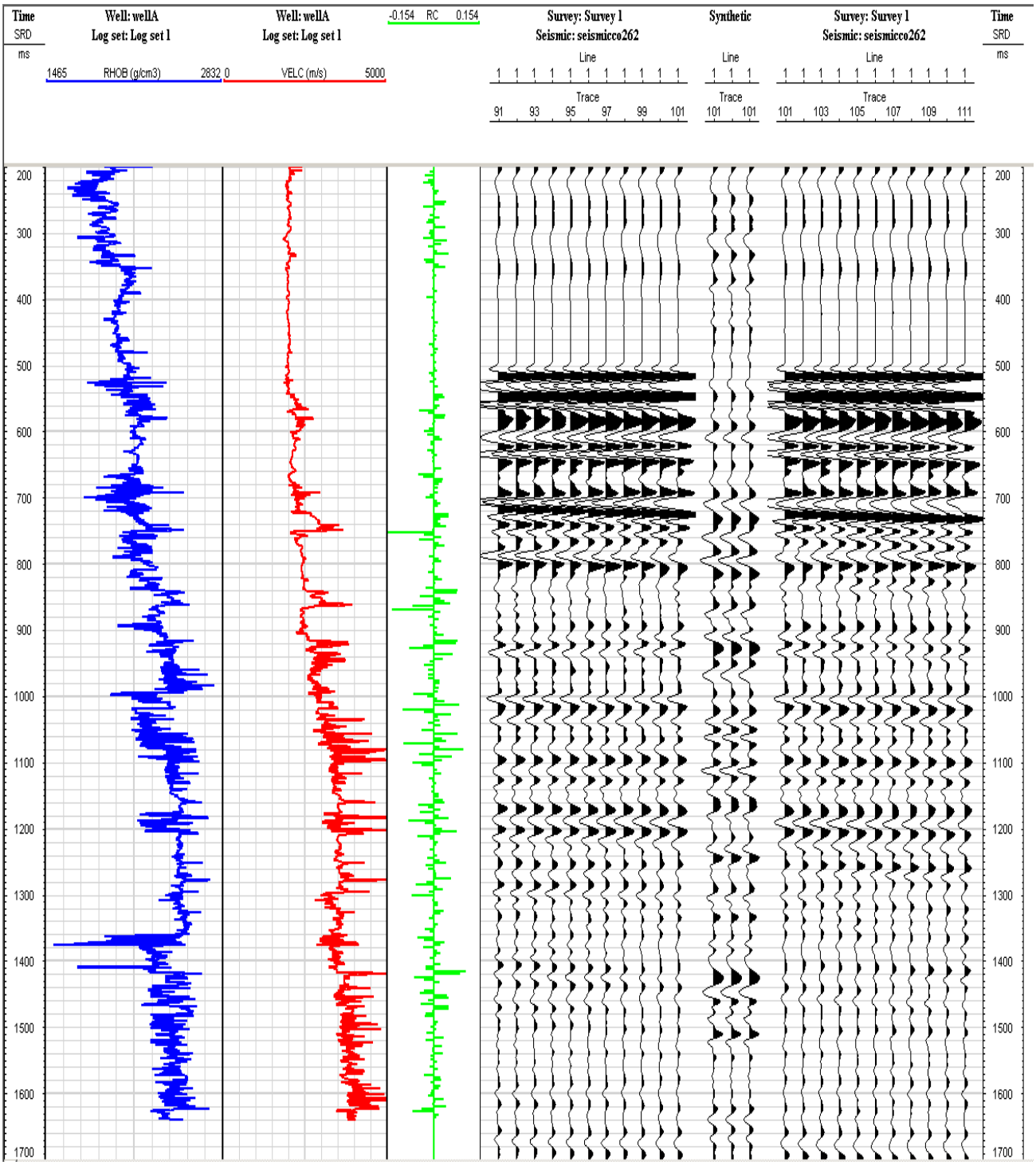


Figure 7 Well Tie Process, from left to right: (a) Density (b) Velocity (c) Reflection Coefficient (d) Seismic trace (e) Synthetic seismic trace based on depth

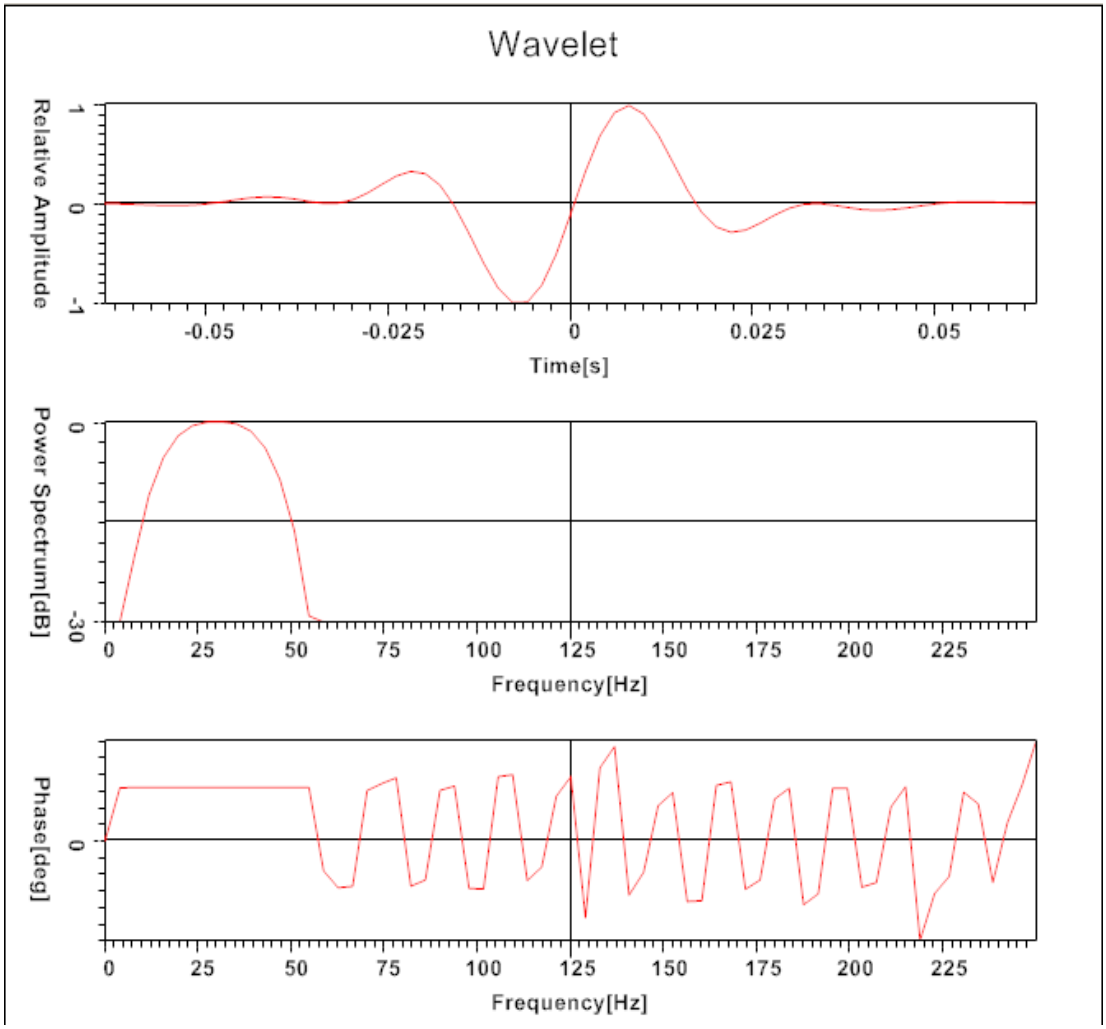


Figure 8 Initial wavelet used in well seismic tie process

A synthetic seismic trace was generated using velocity and density data from Well A (Figure 6), during the procedure of which the reflection coefficient will be calculated using a Ricker wavelet. The synthetic data is generated through Petrel Well Tie Process (Figure 7 and Figure 8). Given the initial synthetic trace, we compare with the real seismic data and change the shape of the synthetic trace (Figure 7). Comparing oil and gas distributions, we could find out that there are two high energy signatures

showing at 2.0s and 2.6s from the distribution (Figure 9).

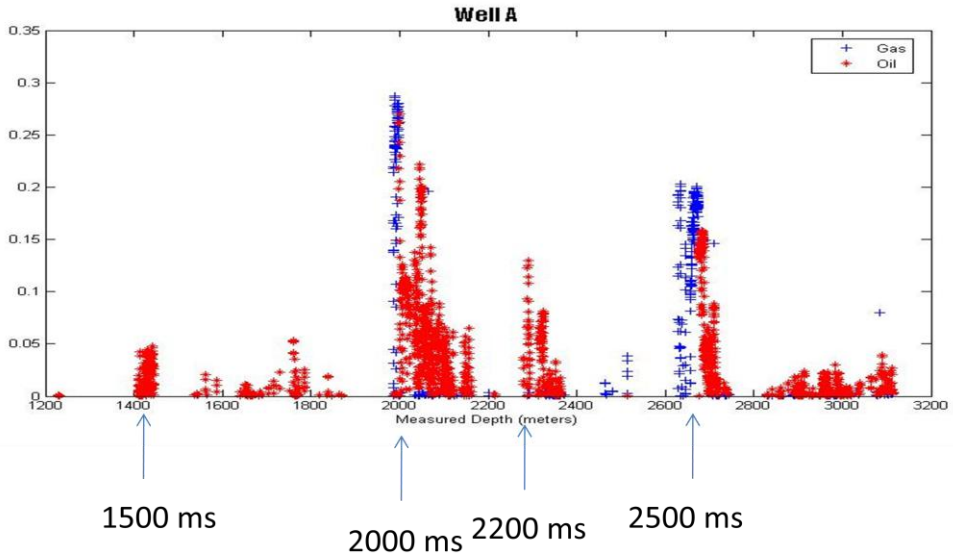


Figure 9 Oil and gas saturation distribution vs. reservoir depth

#### 2.4.1.2 Spectral Analysis on Real Seismic Data Trace

As the oil and gas saturation distribution has been determined in the time domain, the spectral decomposition techniques will be applied to the real seismic trace in the following tests. The analysis of the seismic trace for fluid detection depends upon the amplitude spectrogram, i.e., the energy map of the signal in the time-frequency domain. Because the strong amplitude signal occurs at the beginning due to spherical spreading, it is necessary to take the dynamic equalization of the original data to remove the effect of amplitude variation due to spherical spreading on the seismic trace. This can readily

be done by applying the following relation:

$$f(t) = af(t) / \sum_{k=0}^{a} f(t+k)$$

Here, f (t) is seismic value at time t and ‘a’ is the size of the window.

Figure 10 presents an example of spectrogram of Well A. In the spectrogram, we can observe the decrease of the bandwidth with time due to the absorption. In Figure 10, the low frequency high-energy anomalies occur around 15 Hz. These high energy zones locate from around 1.9 to 2.2s and from 2.6 to 2.8s which match the oil and gas distribution illustrated in Figure 9. The trend with a dominant frequency of around 40 Hz and could be used to detect the unconformity layer.

In addition, the seismic data provided by Exxon Mobile is a raw seismic data set which contains multiples and noises. Therefore, there exist unwanted frequency contents in the spectrogram (Figure 10).

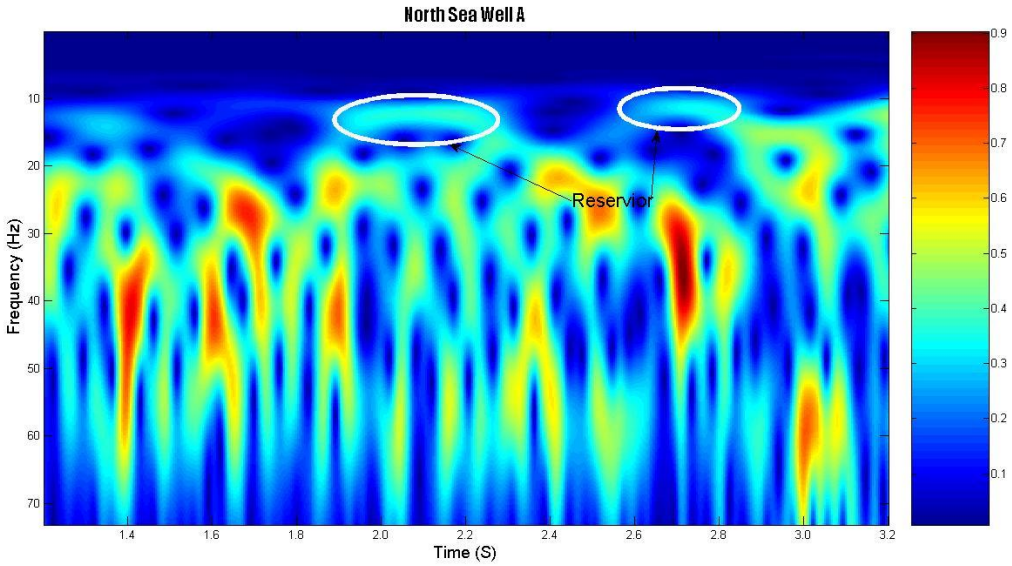


Figure 10 Time-frequency distribution at Well A

In order to confirm the information obtained from spectral analysis of Well A, following the same steps, we analyzed the seismic data at the Well B. Well B contains an interval of oil sands between 2880 and 2950 m. These oil sands are below the Cretaceous unconformity. Gas sands are found below 3200 m in Well B (Figure 11).

Figure 11 shows the oil and gas distribution in Well B. A synthetic seismogram is generated using the density and velocity logs in Well B and Figure 12 shows the time-frequency spectrogram of the synthetic seismogram at Well B location. In the periods of 2.6 to 2.7s, 2.8 to 2.9 and 3.05 to 3.15s, which are related to the locations of the oil and gas reservoirs according to synthetic data, the amplitude of low frequencies turn to high. The low frequency of the high energy zone is around 18Hz and this number is higher

than the one from Well A. One possible reason is that the main hydrocarbon of Well B is oil and Well A produces gas and gas would show lower frequency than oil. Another observation is that the dominant frequency is around 40 Hz and is similar to Well A data.

The information obtained from these two spectrograms matches both predictions and petro-physical log data. Therefore, further steps could be taken with this unprocessed North Sea data for the spectral analysis project.

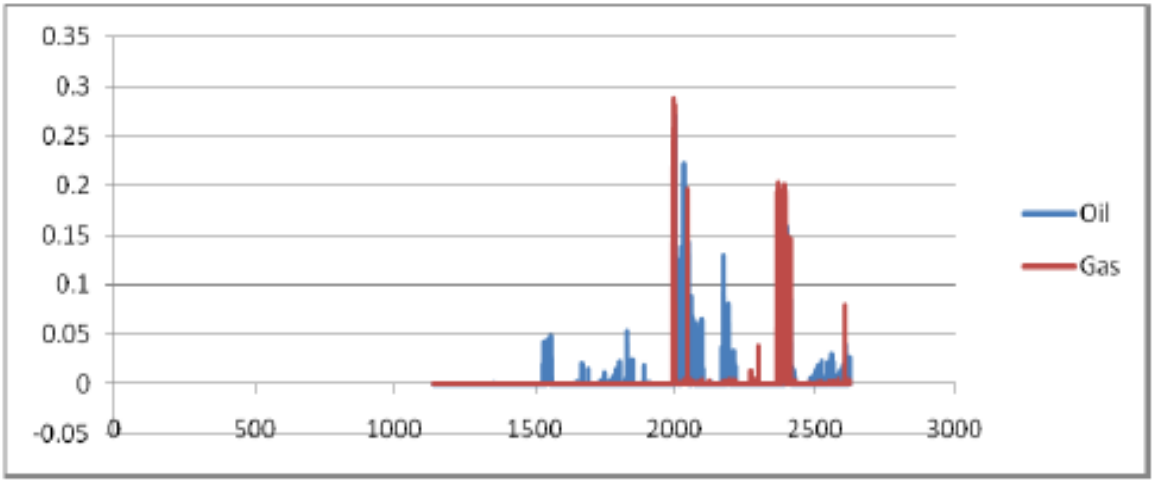


Figure 11 Oil and gas distribution at Well B

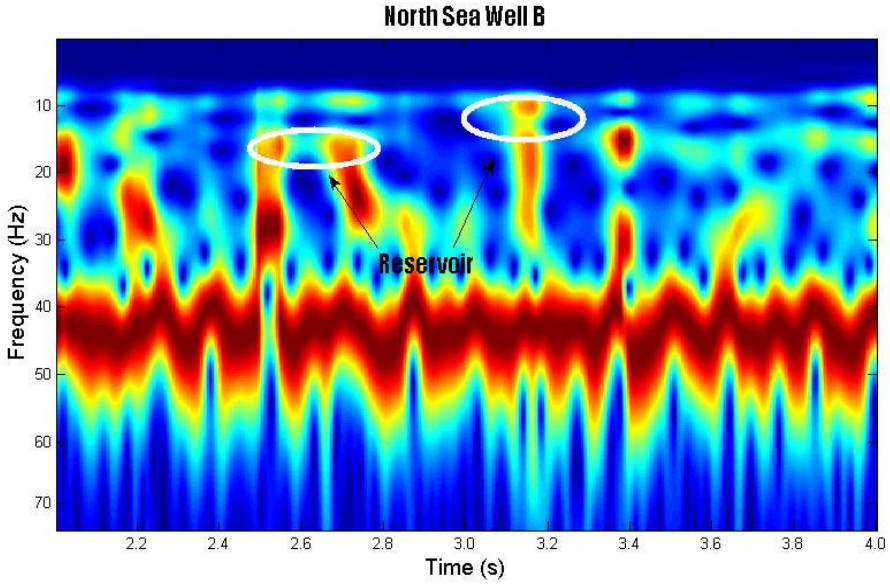


Figure 12 Time-frequency distribution at Well B

#### 2.4.1.3 Analysis on Isofrequency Panel

To apply the spectral decomposition method in the entire 2D seismic section, we decomposed 1001 traces in this cross section individually and then sorted the data into common frequency gathers. Isofrequency spectrogram analysis was done from 10 to 60 Hz using 5 Hz step. In the following sections, we describe the more interesting spectral anomalies.

The 10 Hz spectrogram panel derived from 1.4s to 3.2s is shown in Figure 13. The high-amplitude-low-frequency zone begins to shows up in Well A and Well B around 2.6 to 3.0 s. The observation matches the spectrogram results of Well A and Well B. As the frequency increases, the high energy zones disappear and two obvious trends

show up in the 35 Hz spectrogram panel (Figure 14) which agrees the two lithology unconformities in Figure 5. Not much useful information is shown in the 55 Hz spectrogram panel (Figure 15).

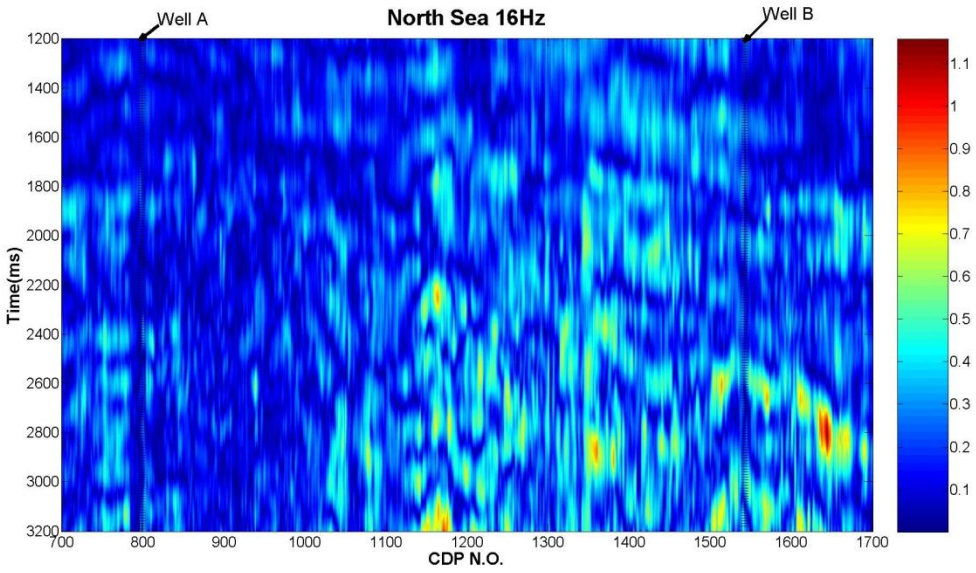


Figure 13 Spectrogram of cross section at 16 Hz

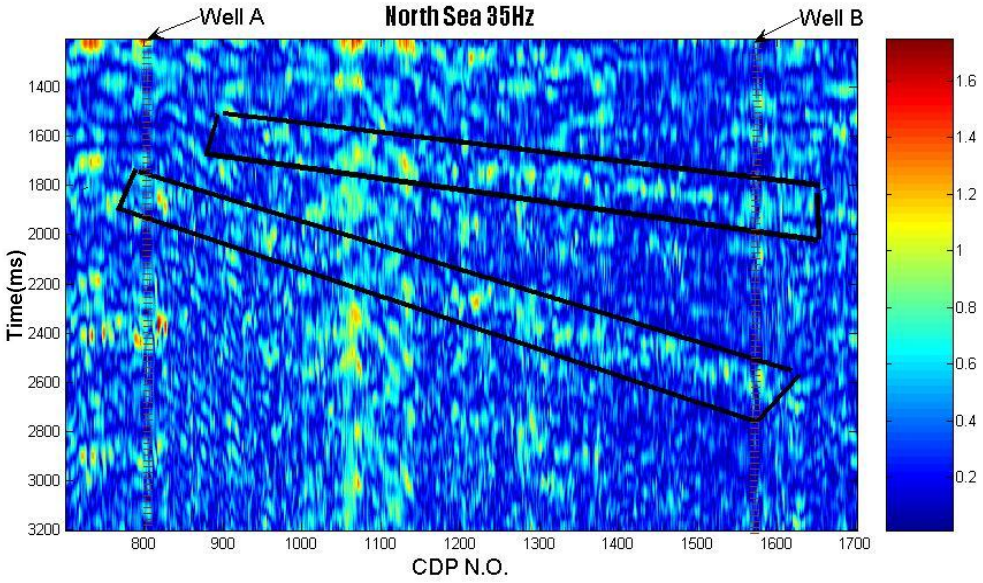


Figure 14 Spectrogram of cross section at 35 Hz

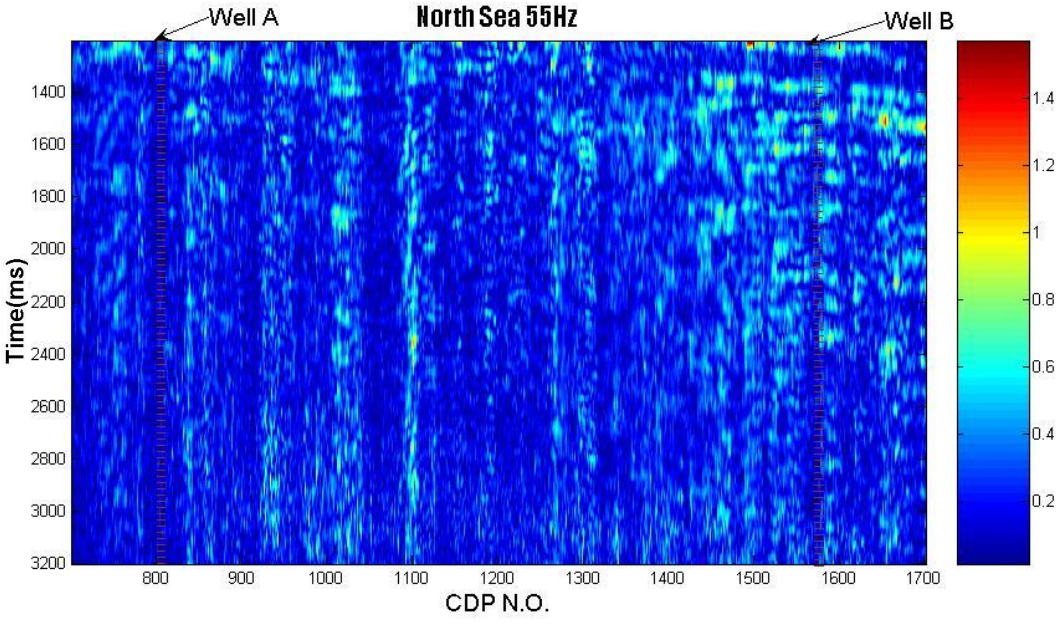


Figure 15 Spectrogram of cross section at 55 Hz

### 2.4.2 Example 2: Yuanba Data Set

Deeply buried gas reservoirs in Sichuan Basin (Figure 16) provide an important future energy resource for China. However, at a depth of about 7km, reservoir rocks are highly pressured and could have porosities as low as 3-5%. The seismic reflection signal is weak and the signal to noise ratio is also low. One of the greatest difficulties encountered is to accurately identify commercial viable targets before drilling. Standard 3D seismic methods for direct hydrocarbon indication have been often proven problematic, if not impossible (Energy News, 2010). Grand challenges and great opportunities in detecting deep gas targets at such great depths are promoted. We attempt to implement spectral decomposition method via S-transform to identify the responses of gas-saturated zones in the time-frequency domain.

This data set is from Feixianguan-Changxing reservoir in Sichuan Basin. The depth of Changxing is around 7154m. It is divided into four intervals based on lithology. They are dolomicrite, micrite, mudstone and intrabiopelmictire. Comparingto Changxing, Feixianguan is deeper. It reaches Jialinjiang and Changxing.

The cross section studied in this section consists of 690 channels for six seconds. The seismic data are sampled every one milliseconds. Three wells, A, B and C, are presented in the cross-section view. The relative position for each wells are labeled respectively (Figure 17). They are Well A (CDP N.O. 5), Well B (CDP N.O. 417) and Well C (CDP N.O. 629). A 3D diagram of decomposed cross section (Figure 18) shows amplitude variance in related low frequency zone. And in the high frequency zone, there is no obvious bright spot shown.

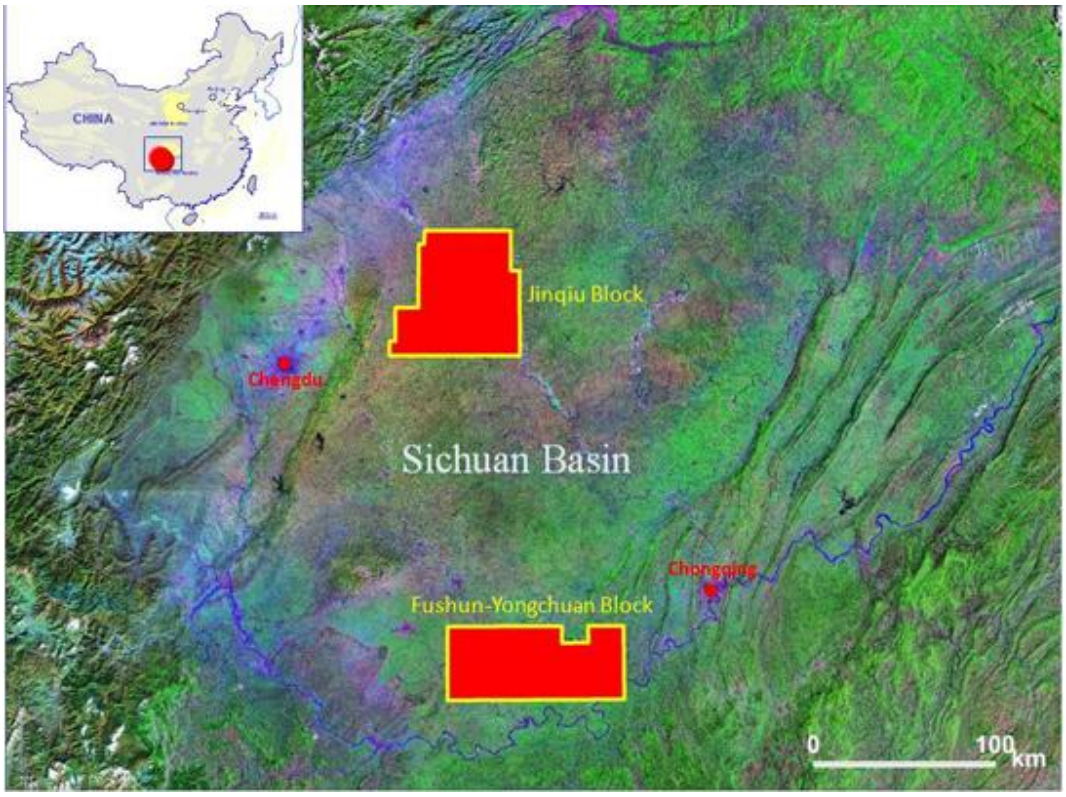


Figure 16 Location of the studied area in the Sichuan Basin (Energy News, 2010)

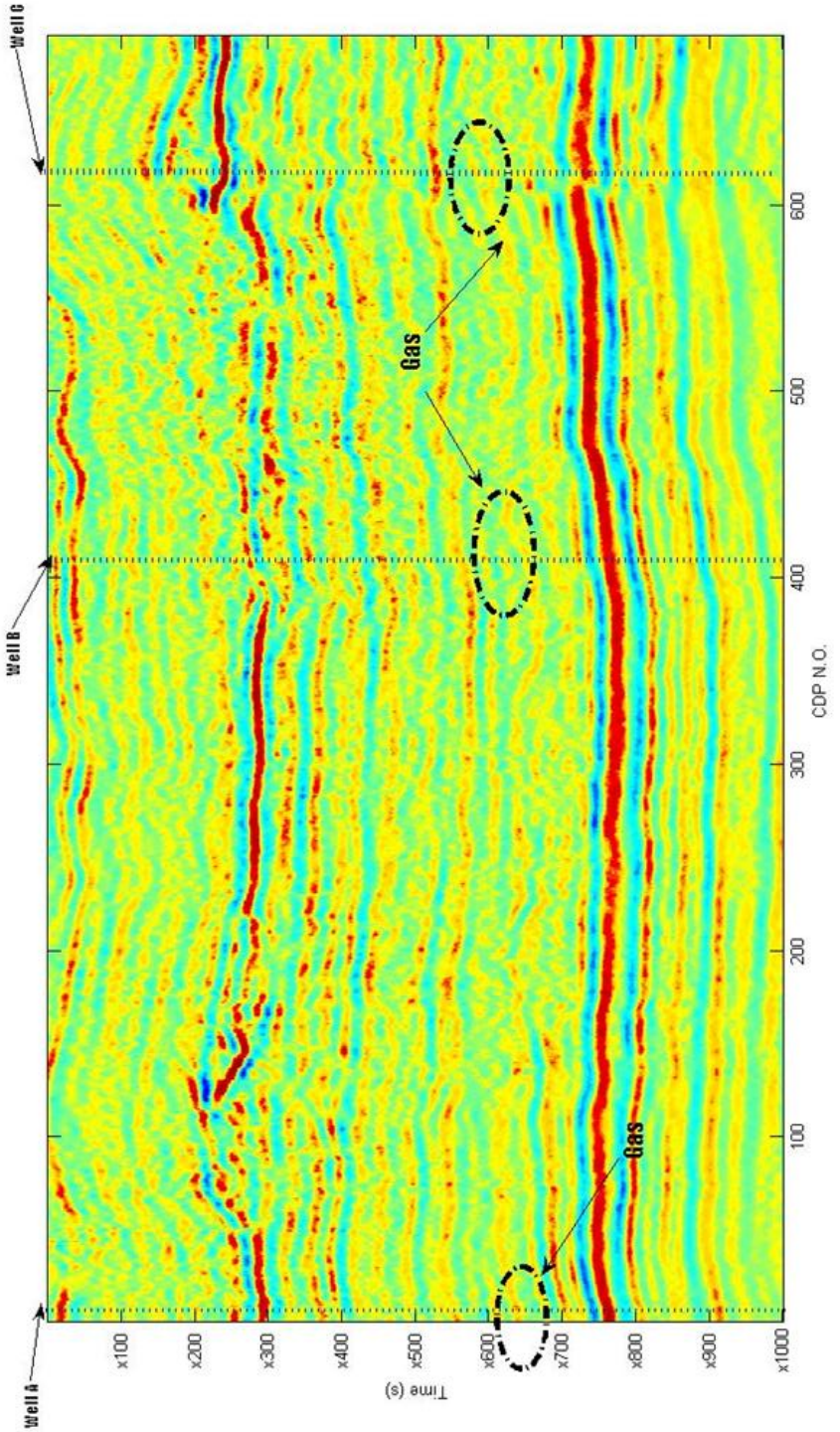


Figure 17 2-D seismic section of the studied area in the Sichuan Basin

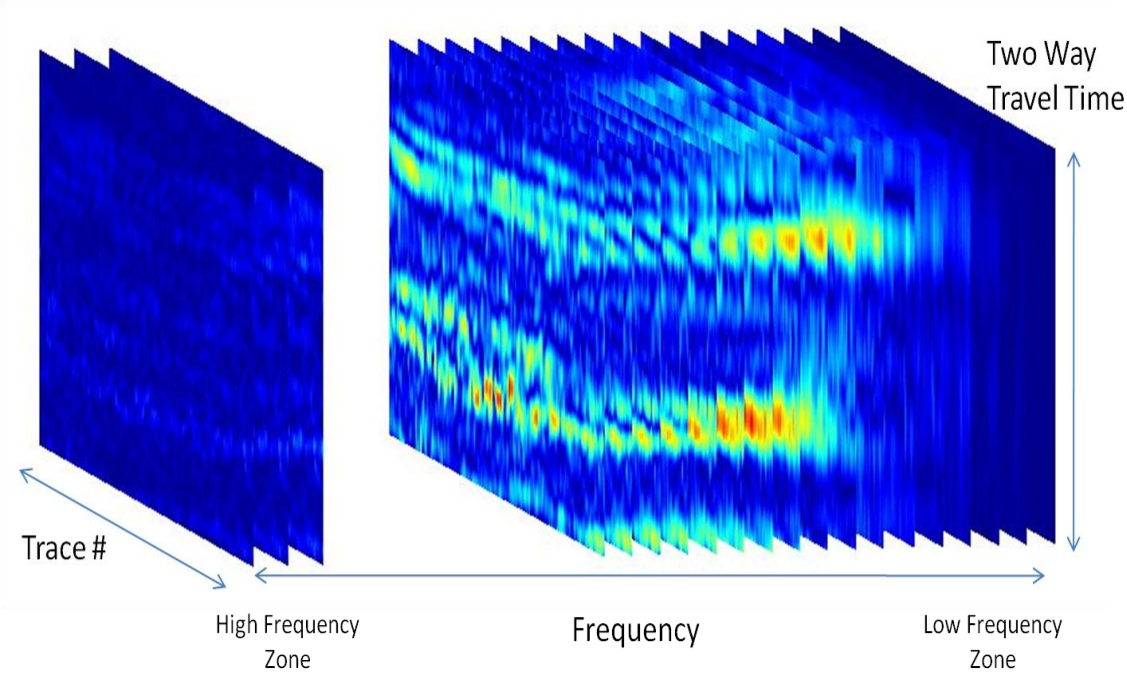


Figure 18 The 3D diagram of decomposed cross section

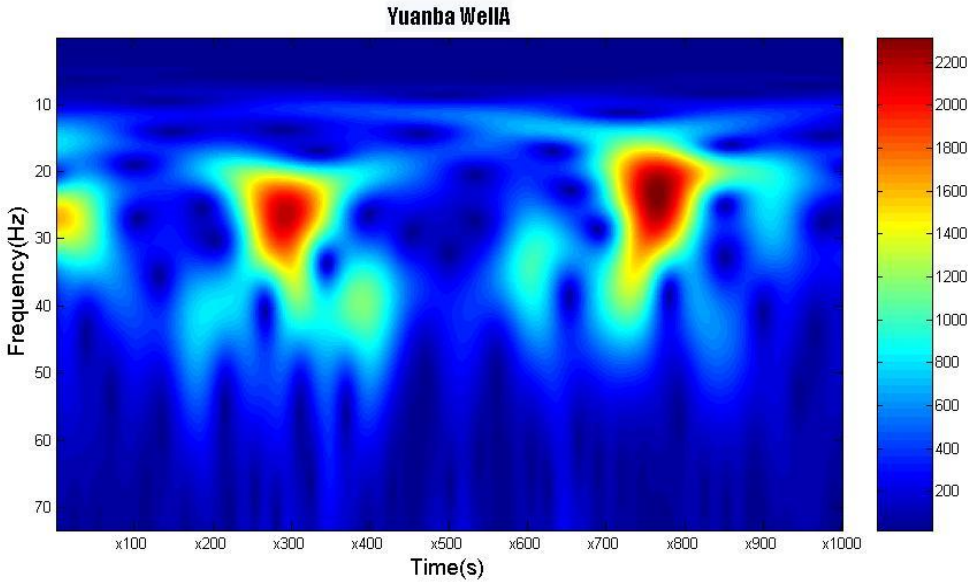


Figure 19 Time-frequency distribution at Well A

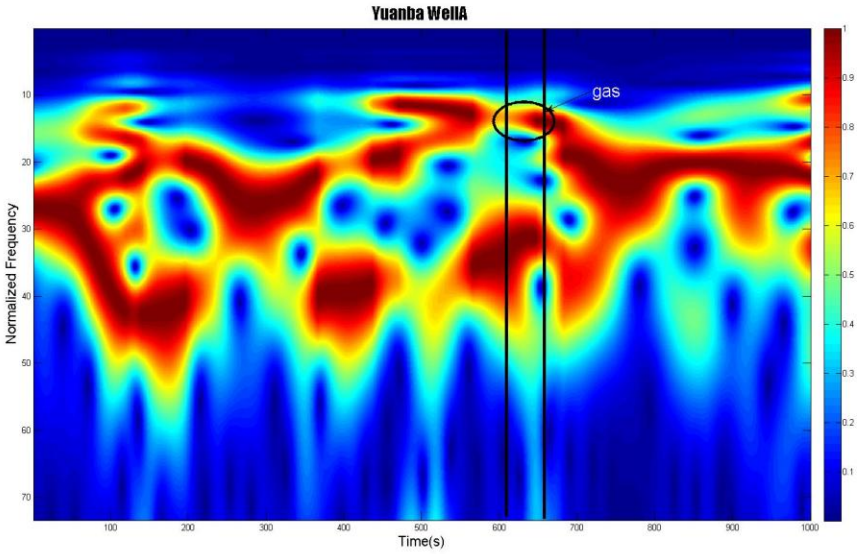


Figure 20 Normalized time-frequency distribution at Well A

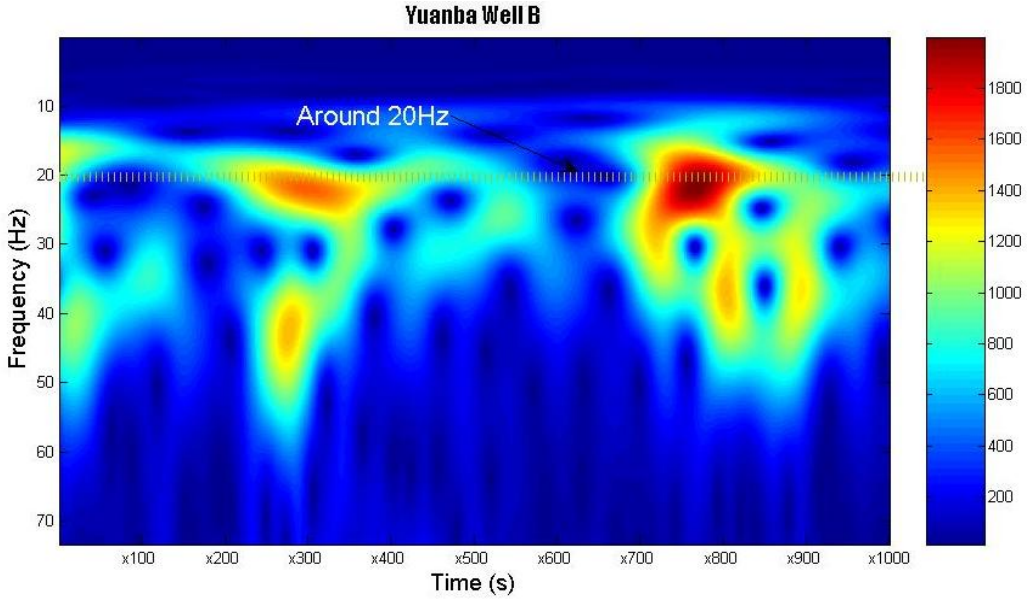


Figure 21 Time-frequency distribution at Well B

The spectrograms of three wells are shown in Figure 19, 21 and 23, respectively. In Figure 19, two strong frequency anomalies show up at x300s and x800s in the frequency zone ranging from 20 Hz to 40 Hz. And, same spectral features exist in Figure 21. The spectrogram of Well C shows frequency anomalies at x200s and x700s (Figure 23) which is lower than those from Well A and Well B. These two frequency anomalies are coming from the reservoir seals which locate at around x200s and x800s in seismic section and show the trends that it is deeper at the location of Well A and lower at Well C (Figure 25).

The bright spots are not obvious in these figures. To amplify the high energy zone, we implement normalization in the frequency domain. The equation is defined as following:

$$g(f,t) = \frac{g(f,t_i)}{Max[g(f_k,t_i)]}$$

where $Max[g(f_k,t_i)]$ is the maximum value in the specific time range.

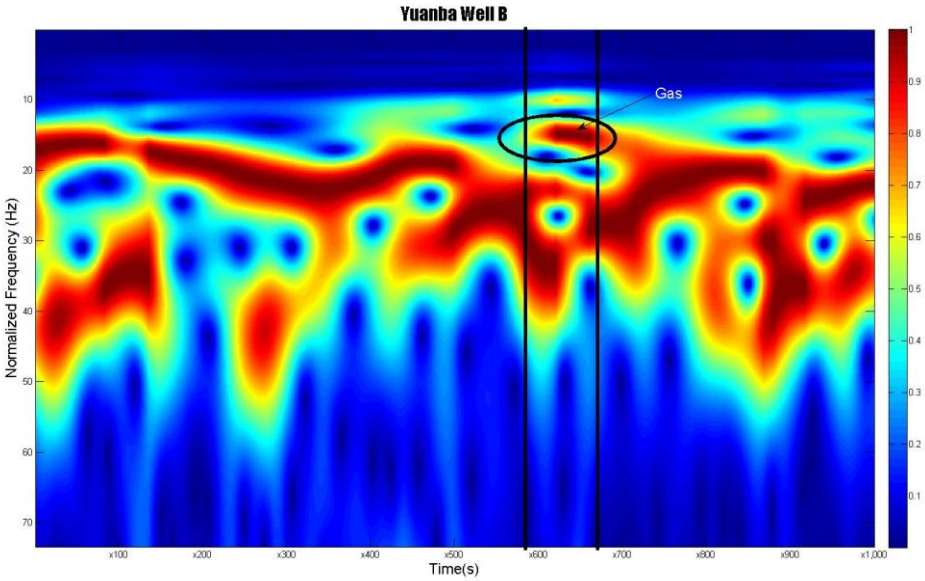


Figure 22 Normalized time-frequency distribution at Well B

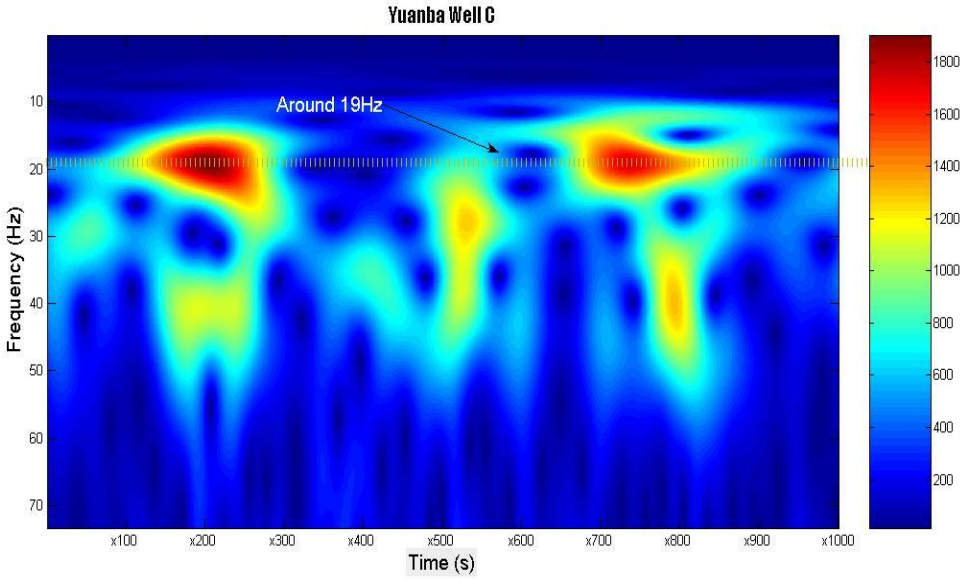


Figure 23 Time-frequency distribution at Well C

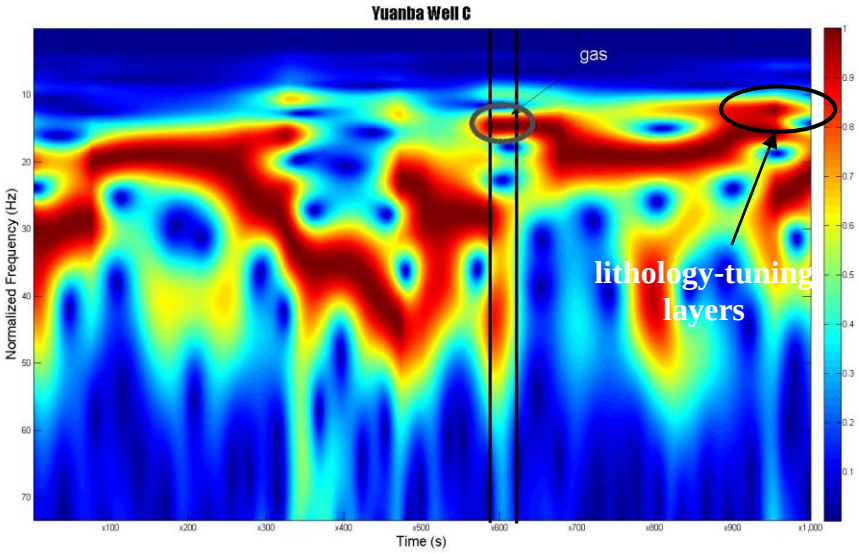


Figure 24 Normalized time-frequency distribution at Well C

In the normalized time-frequency domain, sharp transitions usually occur between the high-frequency anomaly (seal) and the low-frequency anomaly (gas-saturated zone) (Figure 20, 22 and 24). In the Figure 24, there exist frequency anomalies at both x600s and x800s. Compared with seismic section, the tuning of structural beddings shows up at x800s and it is because of the formation changing that high frequency anomaly turns up in the spectrogram (Figure 25). On the other side, there is no structure inconsistent at x600s (Figure 25) where matches the location of the reservoir zone in the seismic data. Same phenomena will be observed in Figure 20 and Figure 22.

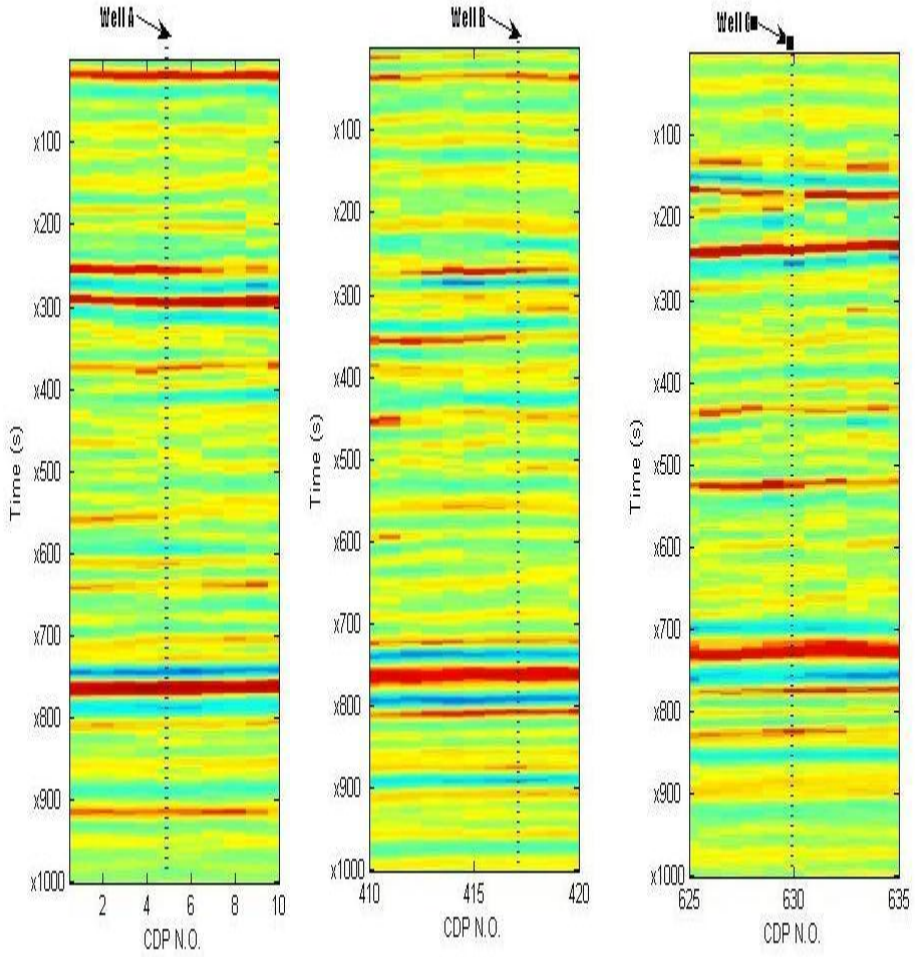


Figure 25 Enlarged parts of the seismic record at Wells A, B and C

After verifying the information from the spectrograms for these three wells, we can apply the continue process of the S-transform to the entire 2D seismic data. A cross section spectrogram is constructed. Figure 26 shows the corresponding spectrogram at 10 Hz. The reservoir is anomalously bright at this frequency. However, the most intriguing finding is that the zone of abnormally strong low-frequency (around x800ms in Figure 26) energy is beneath the reservoir. At 20 Hz the reservoir is clearly defined

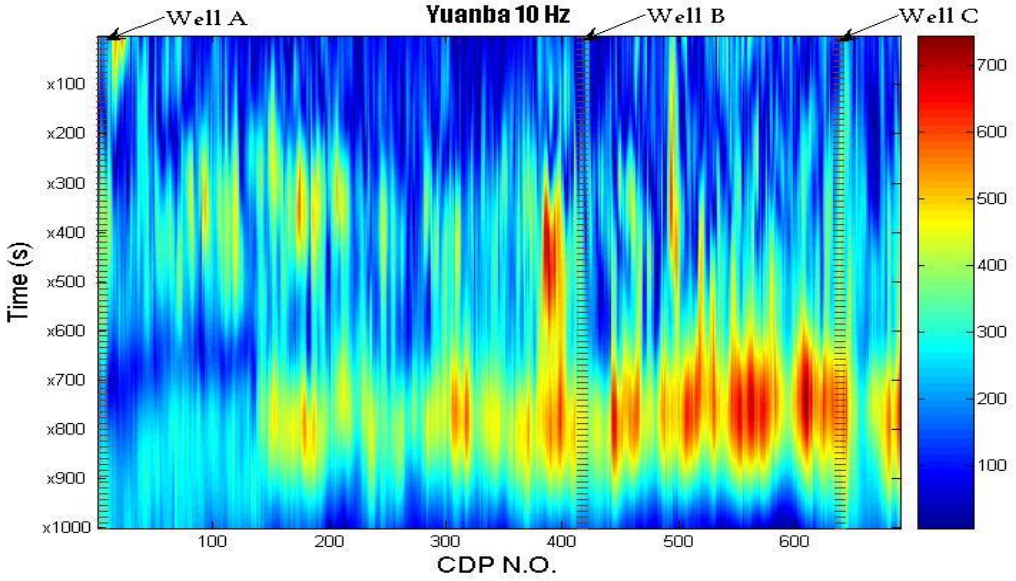


Figure 26 Spectrogram of cross section at 10 Hz

(Figure 27), though less anomalous in amplitude, and the energy under the reservoir apparent at 10 Hz is gone. The shadow has completely disappeared at 30 Hz (Figure 28).

Back to the North Sea data, the frequency anomalies also occur around 20 Hz. We conclude that gas and oil will absorb the high frequency energy and show strong low-frequency energy. Moreover, the low-frequency shadows are much more apparent on spectral decomposed data than on seismic sections.

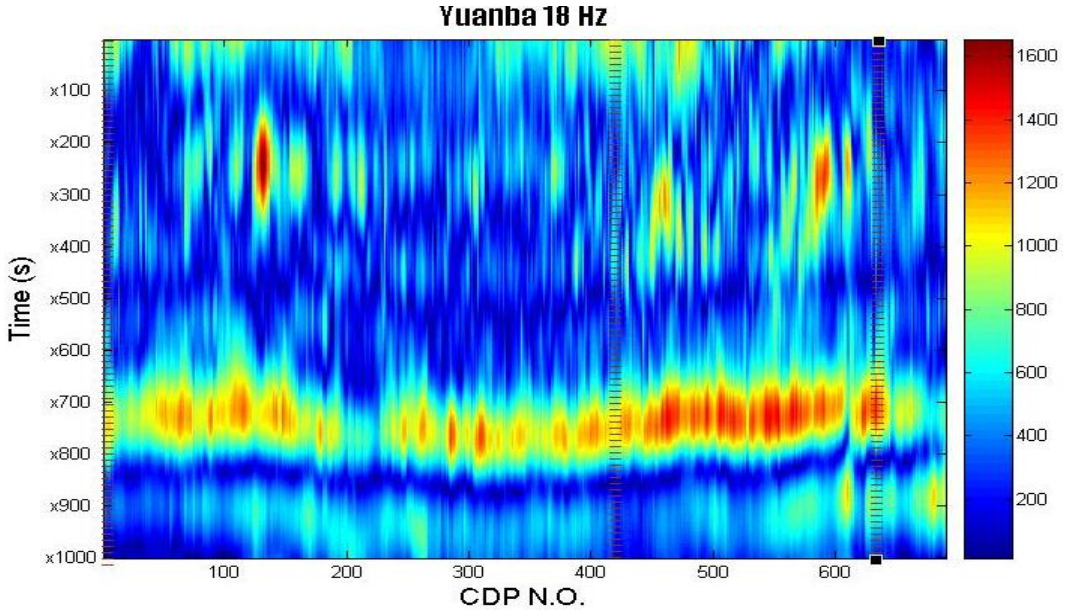


Figure 27 Spectrogram of cross section at 18 Hz

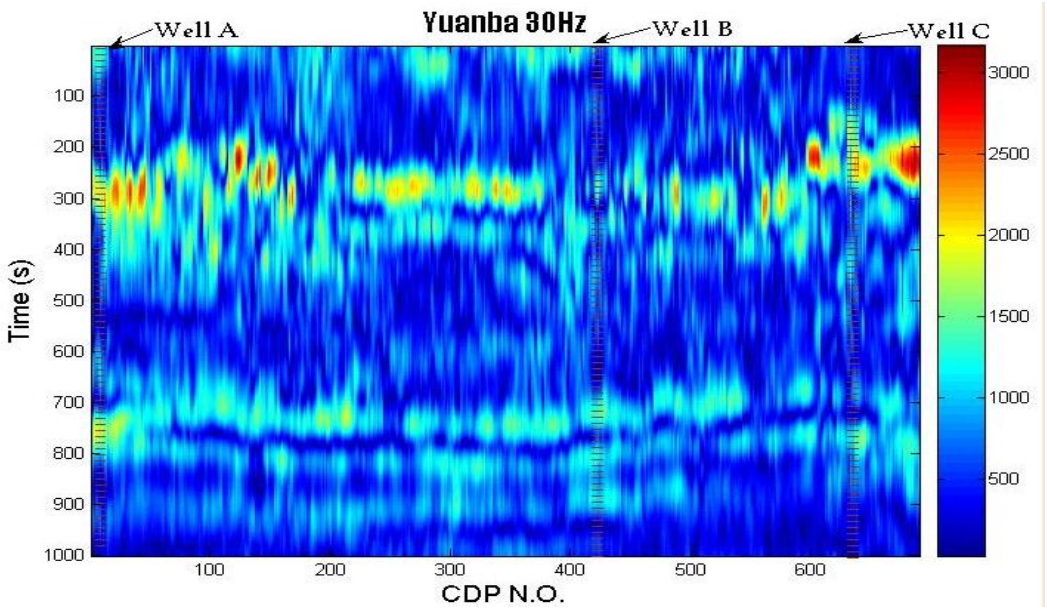


Figure 28 Spectrogram of cross section at 30 Hz

## 2.5 Conclusions

In this part of the work, we implement the spectral decomposition on two real reservoir data sets. During the first process on the reservoir in North Sea area, the signatures of spectrograms fit the background information of real seismic traces. Because of the influence from multiples and noises, there exist unexplained frequency responses. However, high energy zone can still shows at low frequency and the unconformity layer can be observed in corresponding frequency zones. So the spectral analysis is proved as a useful tool to assist geological interpretation and hydrocarbon detection in the clastic type reservoir.

The second application of spectral decomposition analysis is on the super deep gas reservoir in Sichuan Basin. In normalized time-frequency domain, sharp transitions usually occur between the high-frequency anomaly (seal) and low-frequency anomaly (gas-saturated zone). Further separation of gas-saturated zones from lithology tuning needs integrated interpretation of both time-frequency analysis and seismic waveform data in time domain. The apparent frequency of lithology-tuning layers is usually low on seismic section whereas that of a gas or oil zone is not. These findings enable us to improve rock-physics-based quantitative seismic interpretation for deep gas exploration through spectral decomposition analysis.

Therefore, all the evidence confirms that S-transform decomposition analysis technique can be used to assist geological interpretation and hydrocarbon detection in both clastic type reservoir and super deep gas reservoirs.

# 3. SHEAR WAVE ANALYSIS

Surface conditions have great impact on the quality of seismic data collected in the field. Strong surface-wave occurrence and its dispersion create severe problems for seismic data analysis in the shallow water environment of the Persian Gulf where the average water depth is about 10 to 15m. In this area, the velocity of Scholte-waves ranges from 450 m/s to about 2100 m/s depending upon the spatial variation of seabed shear wave velocity. The P-related surface waves usually have a velocity ranging from 1300 m/s to 3500 m/s, which are more severely aliased than other waves in the seismic record (Sun and Berteussen, 2009).

In this section, I demonstrate the application of the S-transform and T-F-K transform to analyze surface waves. It allows the dynamic analysis of surface wave spectrum over time. We could locate and apply a filter to specific time-frequency-wavenumber zones affected by surface waves, leaving the remainder of the trace unaltered.

## 3.1 Introduction

Some important oil and gas fields are in the Persian Gulf where the average water depth could be as shallow as 10 to 15m (Sun and Berteussen, 2009). 4C ocean bottom cable (OBC) seismic data collected in those areas record strong surface waves due to the shallow water depth and hard sea bottom. Sun and Berteussen (2009) showed that the recorded surface waves are spatially aliased and dispersive. Also they represented a

considerable noise problem not only for the actual shot but also for the subsequent shots due to inadequate time delays between shots. The noise causes severe contamination of reflection signals. On the other hand, when the surface waves are measured with sufficient amplitude, its dispersive characteristics can be used to infer the shear-wave properties of the seabed. They could be useful to probe sediment properties of the sea bottom where log data are usually not available. Thus a reliable surface wave analysis tool could be beneficial to hydrocarbon exploration and reservoir characterization of super-giant carbonate reservoirs in the area.

Classical frequency filtering (or windowed frequency filtering) and F-K filtering are two main processing techniques for attenuating surface waves from seismic records. These methods are insufficient in Persian Gulf for two reasons. First, these two techniques are designed in the frequency domain based on Fourier Transform and have the same effect on the whole time series. This brings errors into seismic data processing because seismic data, being non-stationary in nature, has varying frequency content in time. Second, surface waves are highly dispersed and scattered in the Persian Gulf area causing problems of defining a single, appropriate reject zone on the f-k panel. In addition, a combination of spatial aliasing and inadequate delays between shots challenges data processing (Sun and Berteussen, 2009). Thus, an advanced data analysis tool is designed for shallow water environments.

### 3.2 Frequency Filtering

This is the oldest and most common type of filtering. In many cases, frequency

filtering is implemented before the signal is amplified. For the dynamic range of the recording system is limited, simple frequency filtering is not enough for surface waves analysis. Surface waves generated by the shot have large amplitudes which are much larger than those from the desired reflections. Moreover, these amplitudes exceed the dynamic range of the system, causing distortion and loss of the desired linearity of the system. Lowering the sensitivity of the system is undesirable, because this method could also decrease the amplitude of the desired signals.

### 3.3 F-K Filter

F-K filter transform separates the original overlapping seismic events on the basis of their dips. These operations are in the frequency and wavenmber domain. Suppose that the detectors are equally spaced to form a linear array and the signal arrives at different time on adjacent detectors, the filter is designed to pass the signal without distortion while rejecting the noise.

First, consider f(x, t) as a function of x alone and t as one parameter and apply the Fourier transform, then we have:

$$F^*(k,t) = \int_{-\infty}^{\infty} f(x,t) e^{-2\pi j k x} dx$$

.

Next, consider F*(k, t) as a function of t alone with k as the parameter, then:

$$F(k, f) = \int_{-\infty}^{\infty} F^*(k,t) e^{-2\pi j f t} dt$$

Then we have:

$$f(x,t) = \int_{-\infty}^{\infty} \int_{-\infty}^{\infty} F(k, f) e^{2\pi j(ft+kx)} dk\, df$$

And

$$F(k, f) = \int_{-\infty}^{\infty} \int_{-\infty}^{\infty} f(x,t) e^{-2\pi j(ft+kx)} dx\, dt$$

It is assumed that plane waves of the signal have different velocities from those of the coherent noises. From seismic records, signal and noise spectra are obtained and displayed on a graph of frequency versus wave number. Non-dispersive events travelling with a constant velocity are described by straight lines through the origin.

For these assumptions mentioned above, F-K filtering leads to signal distortion and spatial correlation of background noise. It also produces seismic sections of a "wormy" appearance, when applied to real data. Moreover, for the shallow water environment, this problem is more serious. The surface waves are very strong and highly dispersive. The signal band of surface wave affects that of reflection waves. Windowing in the time-offset domain followed by F-K filtering has been used as a method to avoid signal deterioration. However, this method is still computationally expensive and is of limited use for surveys of low-fold coverage.

### 3.4 The T-F-K Transform

A fundamental element of all previous techniques is that they are implemented using the Fourier transform, a method that uses orthogonal basis functions that have perfect localization in frequency but infinite extent in time; therefore, this method assumes that the signal is stationary. This may not be the most appropriate basis dealing

with seismic signals, for which the frequency content is very much time dependent.

Based on S-transform idea, we will design a time varying F-K filter through T-F-K transform. Basically, the data are first transformed from the t-x domain to the t-k domain through 1D Fourier transform over spatial variable, and then are S-transformed over time.

Similar to F-K filter, for a given input signal $u(t,x)$, we first consider u(x, t) as a function of x alone with t as parameter, then:

$$F(k,t) = \int_{-\infty}^{+\infty} u(x,t) e^{-2\pi j k x} dx$$

Next consider F (k, t) as a function of t alone with k as a parameter, then define:

$$F^*(t,k,f) = \int_{-\infty}^{+\infty} F(k,\tau) w(t-\tau, \sigma(f)) e^{-2\pi j f \tau} d\tau$$

The TFK transform is defined as:

$$TFK(t,f,k) = \int_{-\infty}^{+\infty}\int_{-\infty}^{+\infty} u(\tau,x) w(t-\tau,\sigma(f)) e^{-j2\pi(f\tau+kx)} dx d\tau ,$$

where $w(t,\sigma(f))$ is defined as in the previous section. The integration of T-F-K results over time can be regarded as the F-K transform of $u(t,x)$. T-F-K transform appears to have advantages over normal F-K transform when the F-K panel of seismic data varies over time, especially for the data obtained from shallow water environment.

### 3.5 Method

In the F-K domain, various types of seismic events may be separated from one another, compared with the t-x domain representation. The basic idea of separating the surface waves is to filter the unwanted energy on the basis of their dips.

Filtering in time-frequency representation, such as T-F-K domain, can be considered as a procedure of multiplying the spectrum T-F-K(t,f,k) with a filter function H(t,f,k), that is assigned high values to useful signals and low ones to unwanted. Consequently the filtered output time series is:

$$u_{filter}(t,x) = \int_{-\infty}^{+\infty}\int_{-\infty}^{+\infty}\int_{-\infty}^{+\infty} TFK(\tau, f, k)F(\tau, f, k)d\tau \exp(j2\pi ft)df \exp(j2\pi kx)dk$$

We perform our method in the following steps:

1. Apply the T-F-K transform to the original data, and get the 3D result T-F-K (t, f, k) in time-frequency-wavenumber domain.
2. Identify the time-frequency relationship f (t) of surface wave based on specific wavenumber k and the frequency-wavenumber relationship f (k) of surface wave based on specific time t.
3. Design a suitable filter H (t, f, and k) in the T-F-K domain on the basis of T-F (k) and F-K (t) to separate the surface wave.
4. The filtering is imposed on the resulting spectrum within which the undesired energy is zeroed out.
5. Inverse the filtered record through an inverse ST and an inverse FT.

### 3.6 Geology Background

The data analyzed is from Persian Gulf, in southwest Asia (Figure 29). It is an extension of the Indian Ocean located between Iran and the Arabian Peninsula. This inland sea of some 251000 $km^2$ is connected to the Gulf of Oman in the east by the Strait of Hormuz; and its western end is marked by the major river delta of the Shatt al-Arab,

which carries the waters of the Euphrates and the Tigris. Its length is 989 kilometers, with Iran covering most of the northern coast and Saudi Arabia most of the southern coast. The Persian Gulf is about 56 kilometers wide at its narrowest, in the Strait of Hormuz. The waters are overall very shallow, with a maximum depth of 90 meters and an average depth of 10 meters.


Figure 29 Location of the studied area in the Persian Gulf (Radio, 2010)

The Persian Gulf and its coastal areas are the world's largest sources of crude oil and related industries are dominating in this region. Al-Safaniya, the world's largest offshore oilfield, is located in the Persian Gulf. Large gas finds have also been made with Qatar and Iran sharing a giant field across the territorial median line (North Field in the Qatari sector; South Pars Field in the Iranian sector).

However, 4C ocean bottom cable (OBC) seismic data collected in those areas recorded strong surface waves due to the shallow water depth and hard sea bottom. The recorded surface waves are spatially aliased and dispersive.

### 3.7 Data and Modeling Analysis

A 2D 4C OBC data set used for this analysis was acquired in the Persian Gulf where the locale has a very shallow water depth of about 10 m and a hard bottom with P-wave velocity varying from 3 to 4.8 km/s (Sun and Berteussen, 2009).

Figure 30 shows part of a hydrophone record from this data set. The maximum offset of the field data is 10km. The receiver interval is 25m and the recording length is 6 seconds. Surface waves existing in this marine data are trapped waves in the water column and interface waves generated in hard sea-bottom. It displays very strong Scholte waves (Label A, D in Figure 30), P-related interface waves (Label B in Figure 30) and reflected waves (Label C in Figure 30) which all influence the interpretation of reflection events. Because of the very shallow water depth, the Scholte wave keeps rolling for a very long time which represents a serious problem to the data processing. Both the Scholte wave from the present shot (Label D in the Figure 30) and the previous

shot (Label A in the Figure 30) present in the shot record. We also note that the velocity of the Scholte wave. After zooming in the middle part of the shot record (the red square in the Figure 30), we notice the Scholte waves still present a very low velocity (as shown in Figure 31). The reason for this phenomenon is difficult to speculate.

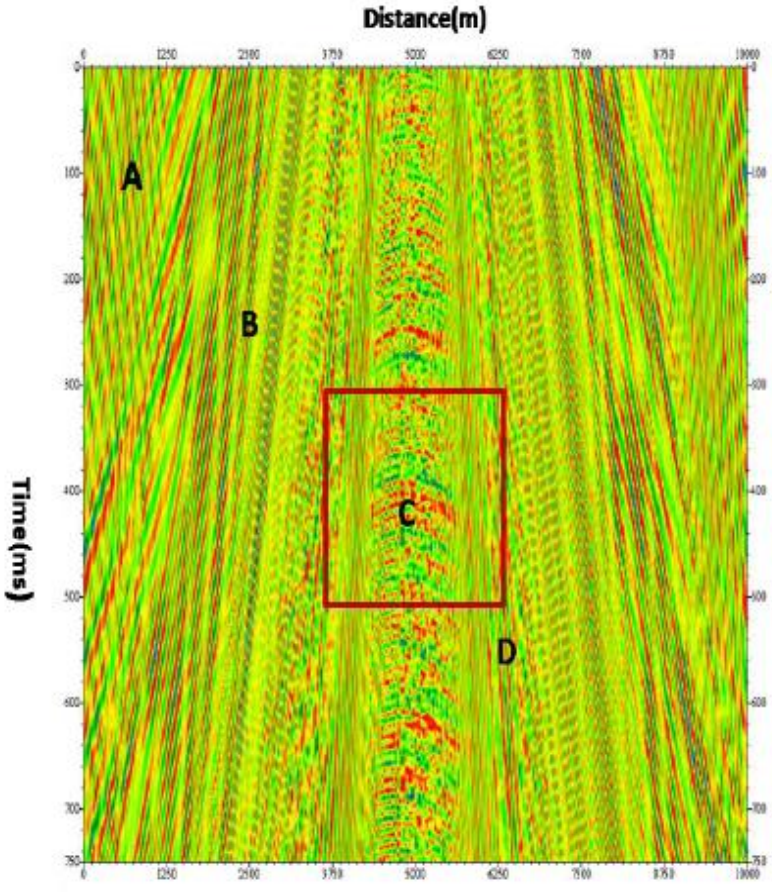


Figure 30 Portion of a typical hydrophone shot gather in the Persian Gulf

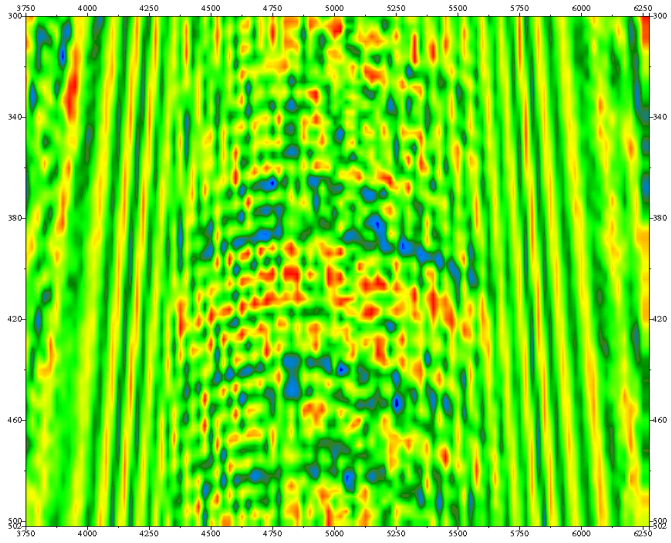


Figure 31 Enlarged portion of the record given in Figure 30 showing surface wave contamination of reflected signals

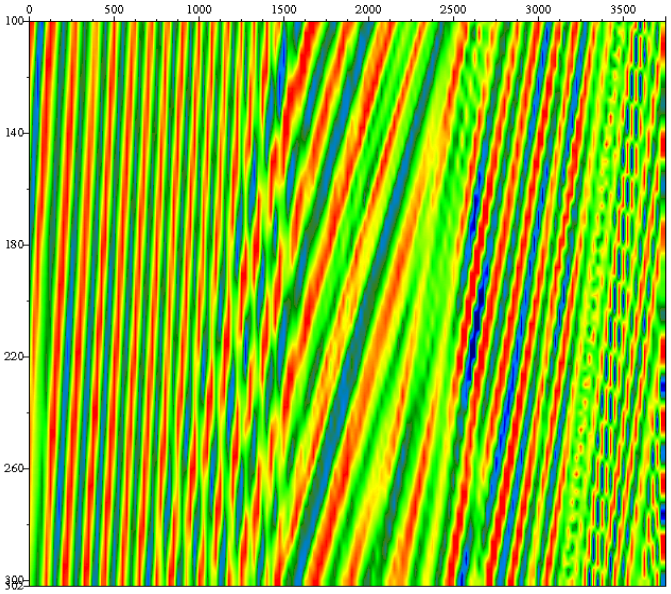


Figure 32 Enlarged portion of the record given in Figure 30 showing surface wave

Figure 33 indicates the T-F-K transform of the record in Figure 30 at time 600ms. Different seismic events are obviously separated. The dominant frequency of Scholte waves is relatively low (less than12 Hz). However, the dipping events are curved instead of straight lines in the F-K domain (the curved line in Figure 33), meaning that the velocity of the Scholte waves is dispersive in the shallow environment. The velocity of Scholte waves is in the range from 450m/s to 2100m/s. The dominant frequency of P-related interface waves is in the range from 20 Hz to 50Hz. However, the spatial aliasing of strong surface waves affects the signal band of reflected waves (as shown with the red square in Figure 30). For the geometric spreading, the energy will decrease with time and the frequency distribution changes with time. In such case, surface wave extraction can no longer be done by a well-localized filter. Moreover, the frequency-domain and frequency-time domain should be considered separately under such circumstance.

Following the steps discussed in the previous section, we could design the weighting function or the filter F (t, f, k) to extract or remove the surface wave, P-related interface waves and reflected waves separately. The corresponding results are shown in Figure 34, Figure 35 and Figure 36, respectively. Almost no seismic reflection has been removed (Figure 36) and surface wave are extracted (Figure 34 and 35). The reflections are clearly visible inside the Scholte wave zone because of a good separation between surface wave and reflection energy in the frequency domain. Two parts of the Scholte waves are exstracted (Figure 34) and the very low velocity part also is presented.

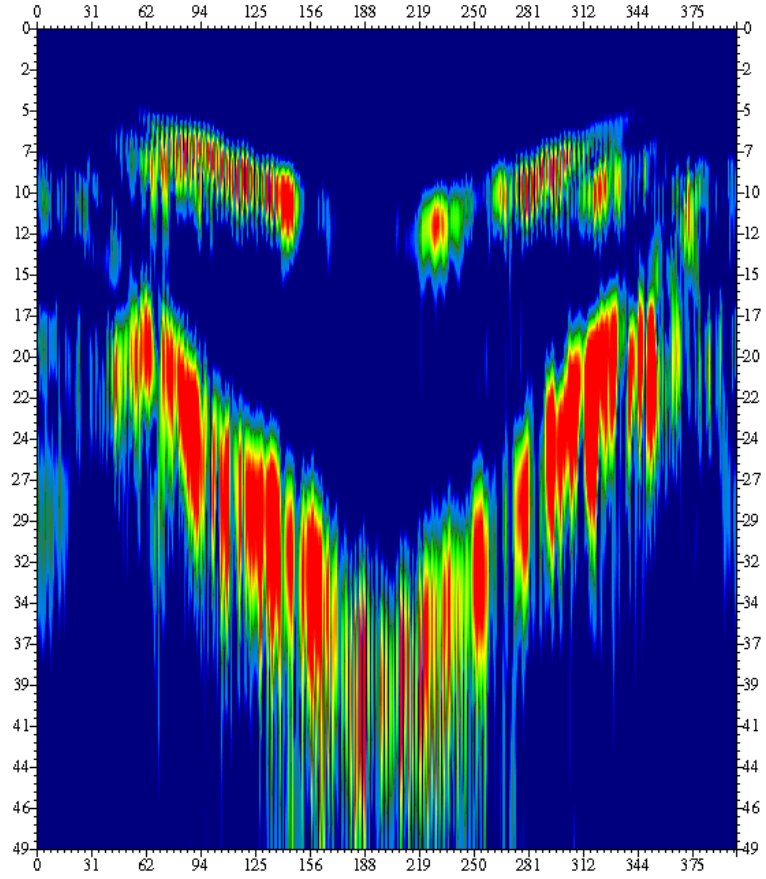


Figure 33 A F-K spectrum at t =600ms

Surface wave dispersion arises because of the velocity stratification of the Earth's interior, longer wavelengths penetrating to greater depths and hence sampling higher velocities. A good extraction of surface wave brings the chance to infer the shear-wave properties of the sea bed. Very low velocity Scholte wave strongly occurs in shallow environment. This observation could help us to further study the geological properties of the seafloor sediment via surface waves in shallow water environment.

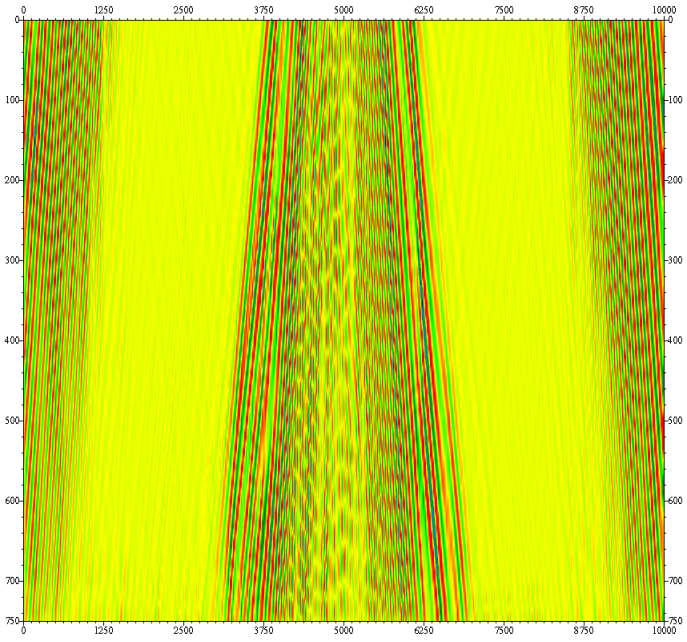


Figure 34 Separated Scholte waves from the record in Figure 30

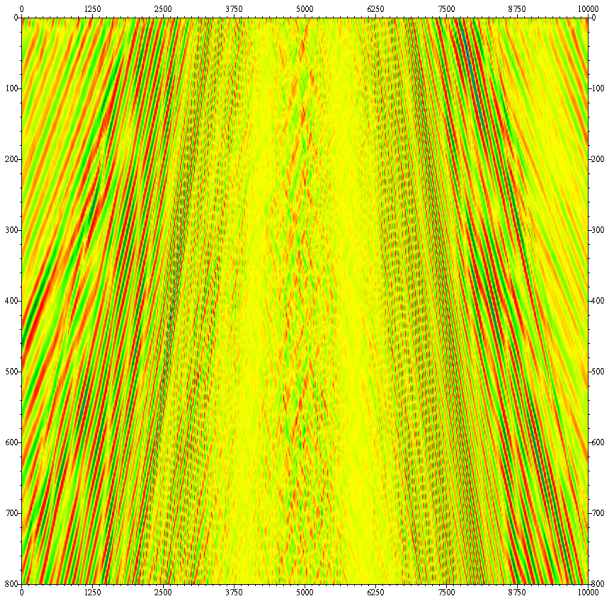


Figure 35 P-related interface waves from the record in Figure 30

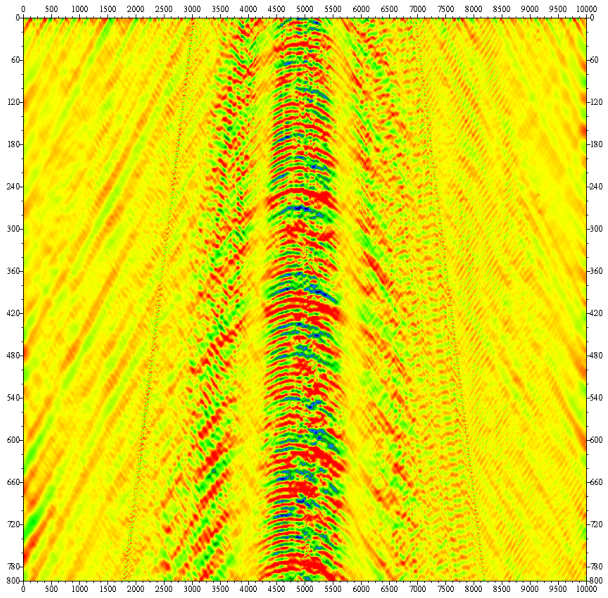


Figure 36 Reflected waves after removal of the surface waves

### 3.8 Conclusions

In this part, we present a time-dependent F-K filter in hard bottom shallow water environments. It filters time varying seismic waves and distinguishes between signals of the same frequency at different times. We implement this method to extract Scholte waves, interface waves and multiple waves from OBS data without removing other seismic signals. In future work, the shear velocity and attenuation properties of the sea beds can be determined through measured propagation characteristics of the surface waves. This method could be helpful for seismic data interpretation and reservoir characterization.

# 4. CONCLUSIONS

Different subsurface structures respond differently to each frequency component of the incident waves. Amplitude and phase spectra of a seismic pulse change during propagation due to attenuation, dispersion and scattering. Spectral decomposition allows us to view subsurface seismic interference at discrete frequencies. This spectral view provides substantially more detail and fidelity than full bandwidth conventional attributes. It reveals stratigraphic and/or structural edges as well as relative thickening and thinning.

Although Fourier transform and short Fourier transform can be used for spectral decomposition analysis, S-transform shows better result theoretically because of its ability of handling the non-stationary seismic wave. Combing the advantages of short-time Fourier analysis and wavelet analysis, S-transform can preserve the phase information in the decomposition and present time-dependent isofrequency profiles. Spectral decomposition using S-transform thus allows a continuous time-varying analysis of the effects of lithology and fluid changes on frequency content.

In my study, I first implement the spectral decomposition method on North Sea data to detect the bright spot. Our results show that for the studied datasets, low-frequency anomalies around 15-19 Hz are usually associated with gas-saturated or oil-saturated zones whereas high-frequency variations are more possible due to oil-saturated zone, anomalies around 30-40 Hz are usually associated with lithology tuning. Then the implementation on a data set from a super deep gas reservoir shows that, in the

normalized frequency time domain, high-frequency anomaly (seal) is due to the tuning of structural beddings and low-frequency anomaly (gas-saturated zone) is rather from intrinsic attenuation and resonance caused by the presence of gas. The result from both data sets demonstrates that the iso-frequency panel on specific frequency could show the oil or gas distribution in the reservoir. Data analysis leads us to believe that this technique might hold a potential to detect hydrocarbon zones by identifying low frequency energy anomalies in the normal trend of frequency decay with depth or two-way travel time.

Then I extend the application of S-transform to filter design. The time-dependent F-K filter could locate the seismic events basing on different time and frequency. It could separate the reflect waves from the Scholte waves and other surface wave in the shallow water environment. This method is used to extract Scholte waves, interface waves and multiple waves from OBS data without removing other useful seismic reflection signals. In future work, the shear velocity and attenuation properties of the seabeds could be determined through measured propagation characteristics of the surface waves. This method could be helpful for seismic data interpretation and reservoir characterization.

# REFERENCES

Askari, R., and H. R. Siahkoohi, 2007, Ground roll attenuation using the S and x-f-k transforms: Geophysical Prospecting, **55**, 1-10.

Beresford-Smith, G., and R. Rango, 1989, Suppression of ground roll by windowing in two domains: First Break, **7**, 55–63.

Castagna, J. P., and S. Sun, 2006, Comparison of spectral decomposition methods: First Break, **24**, 75-79.

Castagna, J. P., S. Sun, and R. Seigfried, 2003, Instantaneous spectral analysis: Detection of low-frequency shadows associated with hydrocarbons: The Leading Edge, **22**, 120-132.

Castagna, J. P., S. Sun, and R. Siegfried, 2002, The use of spectral decomposition as a hydrocarbon indicator: Gas TIPS, Summer, 24-27.

Cohen, L., 1995, Time-frequency analysis: Prentice Hall, Inc.

Daubechies, I., 1992, Ten lectures on wavelets: Society of Industrial and Applied Mathematics, Philadelphia.

Deng, J., D. Han, J. Liu, and Q. Yao, 2007, Application of spectral decomposition to detect deepwater gas reservoir: 77th Annual International Meeting, SEG, Expanded Abstracts, 1427–1431.

Dilay, A., and J. Eastwood, 1995, Spectral analysis applied to seismic monitoring of thermal recovery: The Leading Edge, **14**, 1117-1122.

Ebrom, D., 2004, The low frequency gas shadows in seismic sections: The Leading Edge

**23**, 772-774.

Embree, P., J. P. Burg, and M. M. Backus, 1963, Wide-band velocity filtering-the pie-slice process: Geophysics, **28**, 948-974.

Energy-pedia news, China: International companies set sights on China's natural gas potential, <http://www.energy-pedia.com/article.aspx?articleid=139597>, Assessed September 10, 2010.

Goodyear, B. G., H. Zhu, R. A. Brown, and J. R. Mitchell, 2004, Removal of phase artifacts from fMRI data using a Stockwell transform filter improves brain activity detection: Magnetic Resonance Medvane, **51**, 16-21.

Hlawatsch, F., and G. F. Boudreaux-Bartels, 1992, Linear and quadratic time-frequency signal representations: IEEE Transactions on Signal Processing, **9**, no. 2, 21-67.

Keys, R., and D. Foster, 1998, Comparison of seismic inversion methods on a single real dataset: Society of Exploration Geophysicists.

Miao, X., and S. Cheadle, 1998, High resolution seismic data analysis by wavelet transform and matching pursuit decomposition: Geo-Triad, CSEG, CSPG and CWLS Joint Convention, 31-32.

Miao, X., and W. Moon, 1994, Application of wavelet transform in seismic data processing: 64th Annual International Meeting, SEG, Expanded Abstracts, 1461-1464.

Mitchell, J. T., N. Derzhi, and E. Lickman, 1997, Low frequency shadows: the rule, or the exception?: 67th Annual International Meeting, SEG, Expanded Abstracts, 685-686.

Nawab, S. H., and T. F. Quatieri, 1988, Short-time Fourier transform in advanced topics in signal processing: Prentice-Hall.

Partyka, G., J. Gridley, and J. Lopez, 1999, Interpretational applications of spectral decomposition in reservoir characterization: The Leading Edge, **18**, 353-360.

Peyton, L., T. Bottjer, and G. Partyka, 1998, Interpretation of incised valleys using new 3-D seismic techniques: a case history using spectral decomposition and coherency: The Leading Edge, **17**, 1294-1298.

Pinnegar, C. R., and E. E. Eaton, 2003, Application of the S-transform to prestack noise attenuation filtering: Journal of Geophysics Research, **108**, no. B9, 2422-2431.

Pinnegar, C. R., and L. Mansinha, 2003, The S-transform with windows of arbitrary and varying shape, Geophysics, **68**, 381-385.

Radio Netherlands Wordwide, Britons arrested by Iranian coast guard, <http://www.rnw.nl/english/article/britons-arrested-iranian-coast-guard>, Accessed September 5, 2010.

Stockwell, R. G., 2006, A Basis for efficient representation of the S-transform: IEEE Transactions on Signal Processing, **37,** 371-393.

Stockwell, R. G., L. Mansinha, and R. P. Lowe, 1996, Localization of the complex spectrum: the S-transforms: IEEE Transactions on Signal Process, **44**, no. 4, 998-1001.

Sun, Y. F., and K. Berteussen, 2009, Challenge and opportunity of 4C ocean bottom seismics in shallow water environment, 71st EAGE Conference, Amsterdam, The Netherlands, 8-11 June.

USGS, Viking Graben Assessment Unit 40250101, <http://energy.cr.usgs.gov/WEcont/regions/reg4/P4/tps/AU/au402511.pdf>, Assessed September 20th, 2010.

Zhu, H., B. G. Goodyear, M. L. Lauzon, R. A. Brown, G. Mayer, A. G. Law, L. Mansinha, and J. T. Mitchell, 2003, A new local multistate Fourier analysis for MRI: Medical Physics, **30**, 1134-1141.

# VITA

**Zhao Zhang**

**Address:** Department of Geology and Geophysics
Texas A&M University
College Station, TX 77843-3315

**Education:**

| | | |
|---|---|---|
| B.S. (2008) | Software Engineering, Tianjin University, Tianjin, China |
| M.S. (2011) | Geophysics, Texas A&M University, College Station. |

**Honors:**

| | |
|---|---|
| 2009-2010 | Department of Geology and Geophysics Scholarship, Texas A&M University |

**Selected Publications:**

Zhang Z., and Y. F. Sun, 2011, Identifying lithology variation and gas occurrence in deep carbonate reservoirs using S-transform: AAPG 2011 Annual Convention & Exhibition, 10-13 April 2011, Houston, Texas, USA, 231-232.

Zhang Z, and Y. F. Sun, K. Berteussen, 2010, Analysis of surface waves in shallow water environment of the Persian Gulf using S and T-F-K transform: 80th Annual International Meeting, SEG, Expanded Abstracts, 3723-3727.